COMMERCIAL-IN-CONFIDENCE

COPY NO: _____

AFTS 629/11/14/RPRT-001/ANNEX A

KALKARA FQT LAUNCH FLIGHT DATA AERODYNAMIC REDUCTION

DRAFTED BY: _____
A P Brown, Chief Test Pilot/Chief Aerodynamicist

CHECKED BY: _____
N C Frost, Chief Engineer

APPROVED BY: _
P A Goon, Managing Director

ISSUE:	1	2			
DATE:	16-Mar-99	22-Mar-99			

AMENDMENT LIST NO:	AFFECTED			DATE OF AMENDMENT	DATE OF INCORP'N	INCORPORATED BY
	SECT	PAGE	PARA			
0		-	-			

LIST OF EFFECTIVE PAGES

Page No	Issue No	Amendment No	Amendment Date	Page No	Issue No	Amendment No	Amendment Date
1	2	0	22-Mar-99	24	2	0	22-Mar-99
2	2	0	22-Mar-99	25	2	0	22-Mar-99
3	2	0	22-Mar-99	26	2	0	22-Mar-99
4	2	0	22-Mar-99	27	2	0	22-Mar-99
5	2	0	22-Mar-99	28	2	0	22-Mar-99
6	2	0	22-Mar-99	29	2	0	22-Mar-99
7	2	0	22-Mar-99	30	2	0	22-Mar-99
8	2	0	22-Mar-99	31	2	0	22-Mar-99
9	2	0	22-Mar-99	32	2	0	22-Mar-99
10	2	0	22-Mar-99	33	2	0	22-Mar-99
11	2	0	22-Mar-99	34	2	0	22-Mar-99
12	2	0	22-Mar-99	35	2	0	22-Mar-99
13	2	0	22-Mar-99	36	2	0	22-Mar-99
14	2	0	22-Mar-99	37	2	0	22-Mar-99
15	2	0	22-Mar-99	38	2	0	22-Mar-99
16	2	0	22-Mar-99	39	2	0	22-Mar-99
17	2	0	22-Mar-99	40	2	0	22-Mar-99
18	2	0	22-Mar-99	41	2	0	22-Mar-99
19	2	0	22-Mar-99	42	2	0	22-Mar-99
20	2	0	22-Mar-99	43	2	0	22-Mar-99
21	2	0	22-Mar-99	44	2	0	22-Mar-99
22	2	0	22-Mar-99				
23	2	0	22-Mar-99				

TABLE OF CONTENTS

1. INTRODUCTION

1.1 Purpose

1.1.1 Kalkara AFQT flight data has been reduced, for the purposes of deriving incidence and sideslip envelope data and roll/yaw instability data through the launch phase of flight. The derived data will enable parametric quantification, analysis an evaluation of the flight path excursions and instabilities, experienced by the aircraft, on flight test.

1.2 Scope

1.2.1 By the document date, Kalkara has undertaken twenty qualification test flights at the Jervis Bay Range Facility (JBRF). Aerodynamic data reduction has been conducted for all flights, with the exception of FQT 4.

1.3 References

A. AFTS 808/11/05/PROC-002, Document Control Procedure.

1.4 Amendments

1.4.1 This report is a controlled document, which shall be amended in accordance with the procedures detailed in Reference **Error! Reference source not found.**.

1.5 Glossary of Terms

1.5.1 Abbreviations

DAP	Digital Autopilot
DGPS	Differential GPS
HDG	Aircraft heading
JBRF	Jervis Bay Range Facility
LRU	Line replaceable unit
MAGIC^2	Multiple Aircraft GPS Integrated Command and Control
RATO	Rocket-Assisted Take-Off
VG	Vertical gyro
V_{TAS}	True air speed
u_A,v_A,w_A	Velocity components, in air mass axes (no vertical wind component assumed, in any case)
u_E,v_E,w_E	Velocity component, in earth axes
u_B,v_B,w_B	Velocity components, in aircraft body exes
α	Angle of incidence (angle of attack)
β	Angle of sideslip

2. DATA REDUCTION METHODOLOGY

2.1 Data acquisition

1.1.1 The monitoring and acquisition of flight data is controlled digitally by the MAGIC^2 software data control system. Data is acquired near-real-time via the command telemetry link with the Kalkara flight vehicle, for ground computer storage and subsequent replay/reduction.

2.1.2 Acquired data includes:

a. air data:

(1) static and pitot pressures, from the flight vehicle pitot-static system;

b. inertial data:

(1) attitude and roll/pitch rate data from the flight vehicle vertical gyro (VG),
(2) heading from the magnetometer, yaw rate from the yaw rate gyro,
(3) GPS position and time-base;

c. control status data, including:

(1) engine,
(2) flight controls (elevator and ailerons), and
(3) stores deployment, stowage and release.

2.1.3 Whilst the air and inertial data is acquired at 10 Hz, the DGPS data is acquired and stored at 1 Hz sampling. The following data reduction has been conducted upon 10 Hz sampled data, namely air and on-board inertial data, rather than more slowly-acquired DGPS data. Therefore, the vertical wind component has been assumed to be zero.

2.2 Data reduction methodology

2.2.1 The data reduction methodology has been based upon the following assumptions:

a. zero vertical wind component and zero horizontal wind components;

b. zero pitot tube error, within a semi-cone angle of 15 degrees; and

c. zero static position error correction.

2.2.2 The data reduction process has consisted of:

a. low-pass filtering of pressure altitude, Hp;

b. differentiation of Hp, to derive w_E, $w_A=w_E$ under the zero vertical wind component assumption;

c. ΔHDG and TAS to derive $u_A=u_E$ and $v_A=v_E$ under the zero horizontal wind component assumption;

d. Inverse Euler anglular transformation to derive u_B, v_B and w_B; and

e. Incidence and sideslip formulations from

(1) $\tan\alpha=w_B/u_B$ and
(2) $\sin\beta=v_B/V_{TAS}$.

3. RESULTS AND DISCUSSION

3.1 Kalkara payloads

3.1.1 The following is the range of Kalkara payloads, referenced in the test flight configuration summary:

a. TPT-6A Short IR Tow;

b. AWC-18 Flare Chaff Dispensers;

c. APC-4 Wing Tip IR Pods;

d. TRX-17 Short RF Tow;

e. TRX-17 Short Dummy Tow;

f. TRX-17 Long RF Tow;

g. TRX-17 Dummy Long Tow; and

h. TRX-17 Short Dummy Tow with fore and aft lenses.

3.2 General

3.2.1 The results of the data reduction process are grouped by configurations, as follows (in addition, the following list indicates #, for those FQTs which could have possible inertial asymmetry between left and right wing stores, prior to store mass/CG ballasting being introduced as a normal flight procedure):

a. TPT17RF/TRX17DUMMY: FQT 8#, 9#, 10, 11, 12, 13, 14, 15, 16 and 17;

b. NIL: FQT 1 and 4;

c. TPT-6A x 2: FQT 2# (MRL25A), 5# and 19;

d. AWC18/APC4 x 2: FQT 3#;

e. TPT6A(IR)/TRX17(RF): FQT 6#;

f. TRX17(2LENS) x 2: FQT 18; and

g. WINGTIP&AWC x 2: FQT 20.

3.3 TPT17RF/TRX17DUMMY

3.3.1 FQT 8:

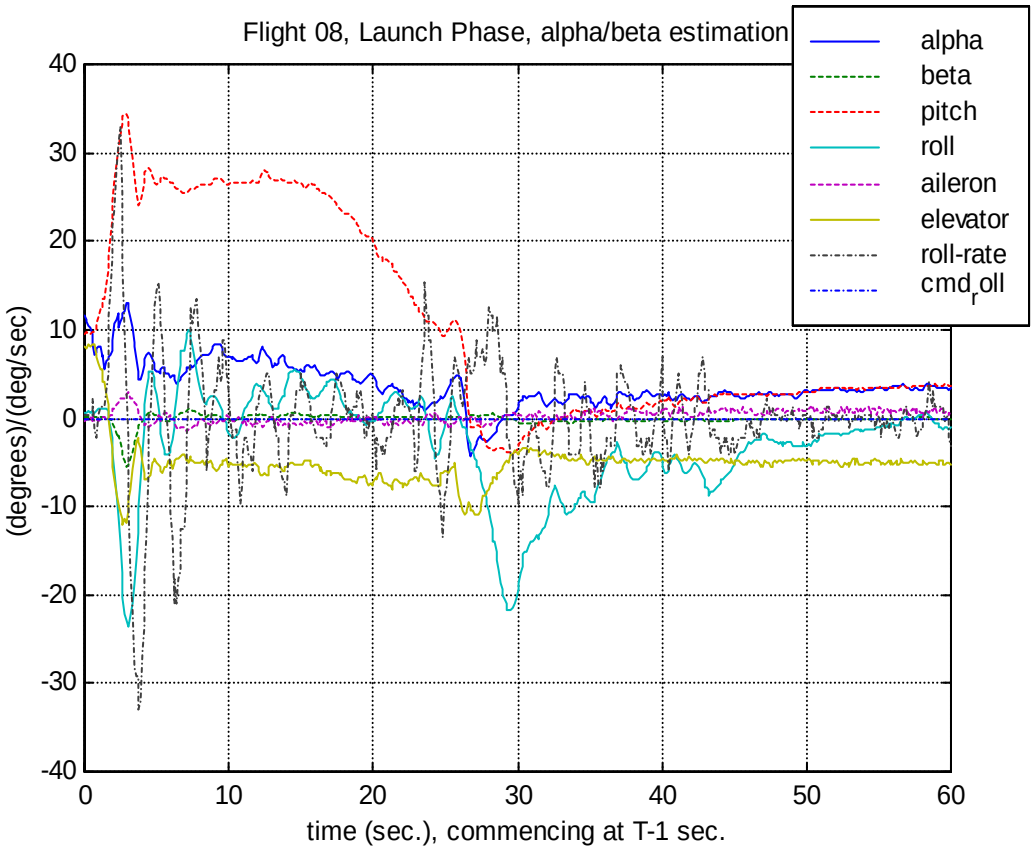

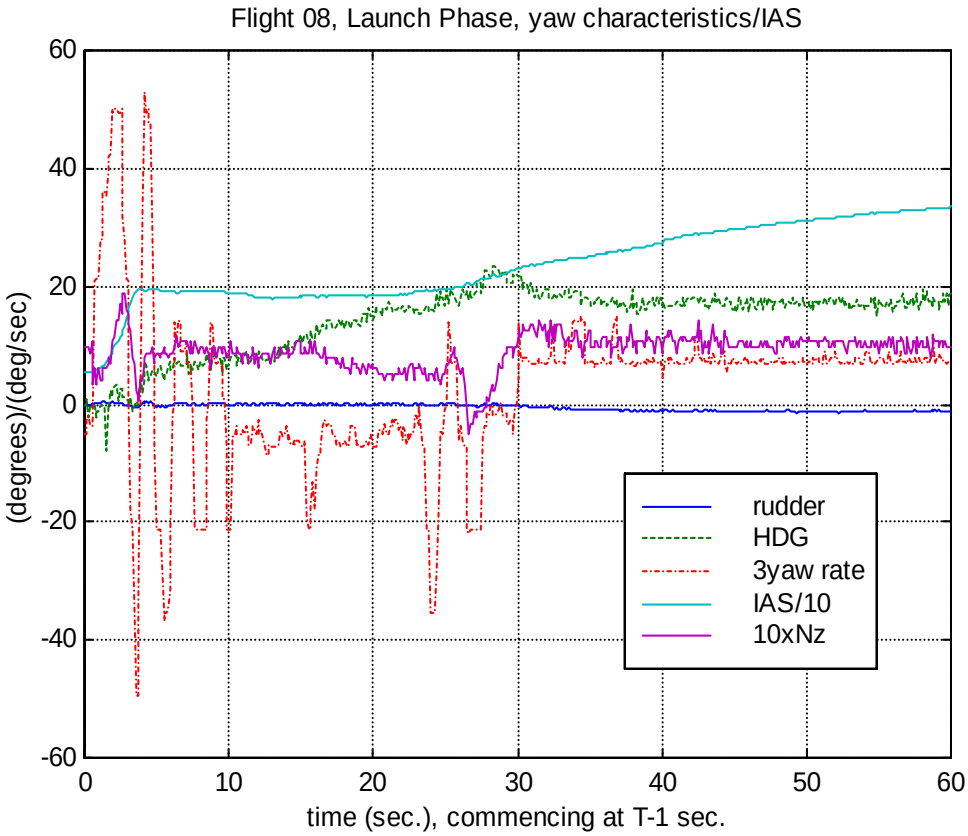

3.3.1.1 Launch-site wind was 120/10 knots, i.e. an 8 knot crosswind from the right. Nevertheless, as seen from the first figure, above, the aircraft exhibited a marked uncommanded left roll, i.e. negative roll damping ,$-L_P<0$, and left yaw. The roll onset occurred with incidence rising through 7°. The DAP commanded aileron deflection arrested the roll, with incidence at a peak of 13°. However, over the period T+4 to T+19 seconds, roll damping varied between neutral and negative, resulting in overshooting roll characteristics.

3.3.1.2 Together with the initial roll, such behaviour is indicative of significant initial and residual wing-flow separation. At the pitch-over completion 'bunt', the incidence peaked at -4.2°, and uncommanded roll occurred, i.e. negative roll damping, $-L_P<0$. Positive roll stability returned, with the assistance of slight DAP-commanded positive aileron deflection, as incidence increased through 0°. Between T+30 and T+42, overshooting roll characteristics continued. Following T+43, monotonic reduction in roll occurred to the null-roll position.

3.3.2 FQT 9:

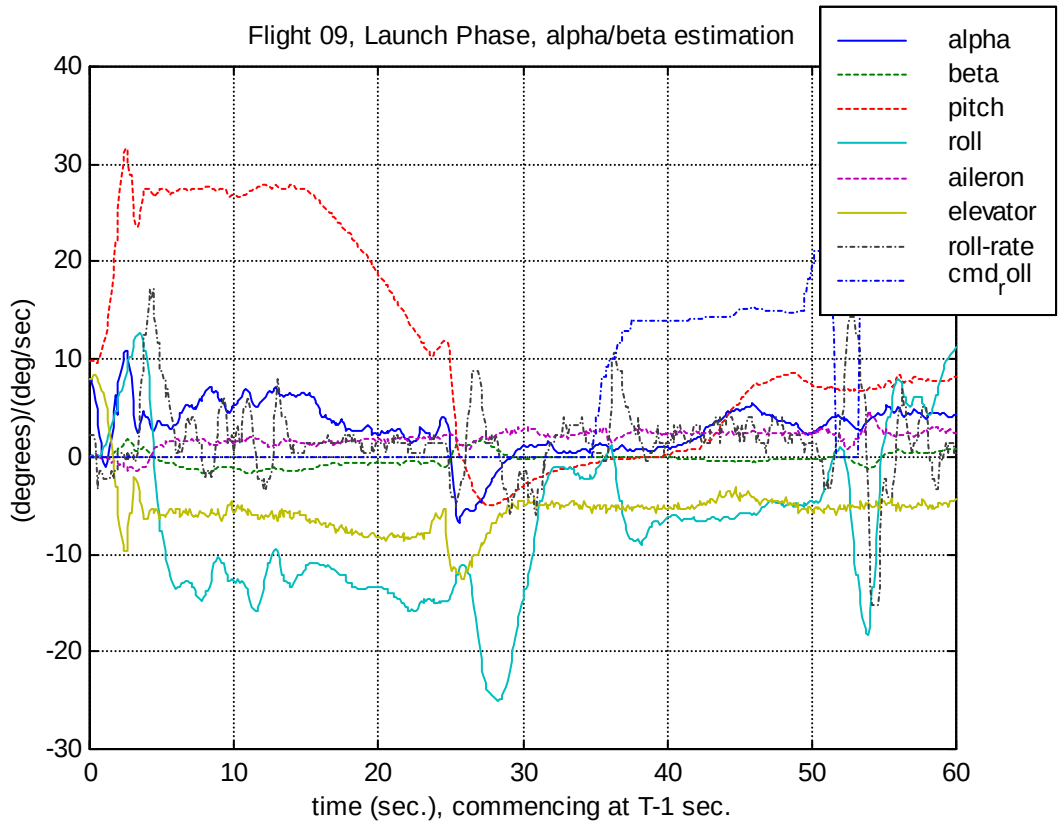

3.3.2.1 At launch, mild roll divergence occurred at a relatively-slow roll rate. The roll preceded the incidence rise, and is likely to be attributable to, either wind conditions or RATO-thrust, rather than to flow separation. The mild roll peaked near RATO-separation and was followed by roll reversal, to -12°, under the initiating action of DAP-applied aileron. Thereafter, aileron was approximately constant, maintaining roll at an offset angle, rather than driving towards the null-roll position, until the pitch-over 'bunt', at which, initially roll reduced, as incidence reduced through 0°, then abruptly reversed in an $-L_P<0$ roll to -25°. Following recovery from the 'bunt', the roll-offset was difficult to null, even under the action of CMD-roll.

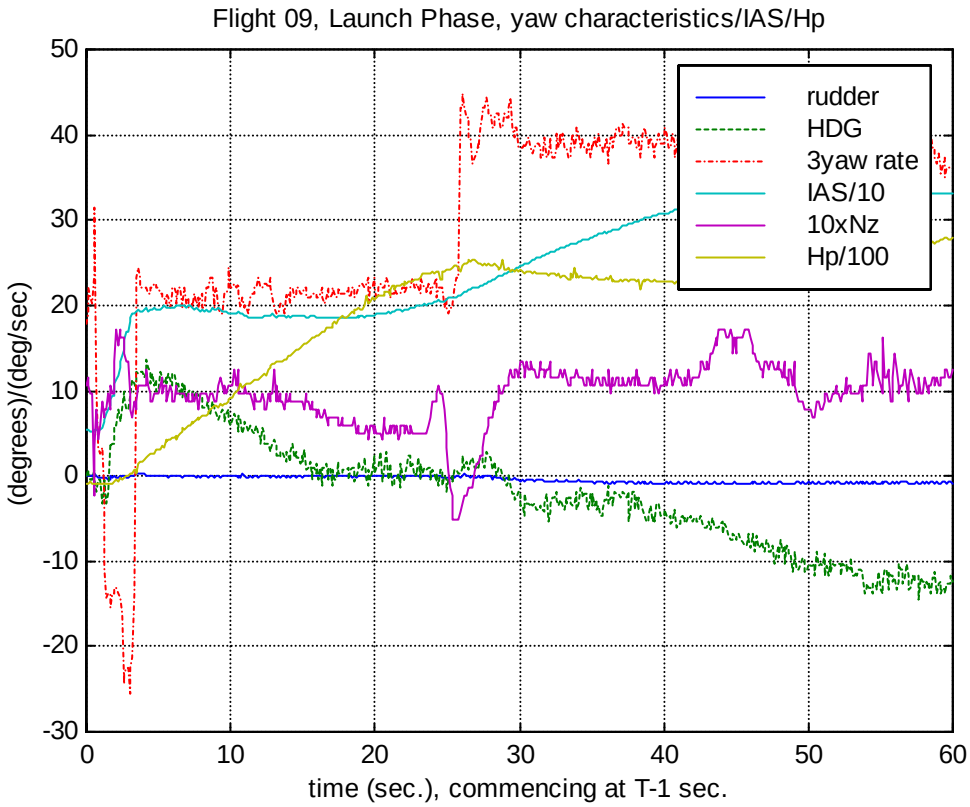
Flight 09, Launch Phase, yaw characteristics/IAS/Hp
rudder
HDG
3yaw rate
IAS/10
10xNz
Hp/100
(degrees)/(deg/sec)
time (sec.), commencing at T-1 sec.
50
40
30
20
10
0
-10
-20
-30
0
10
20
30
40
50
60

3.3.3 FQT 10:

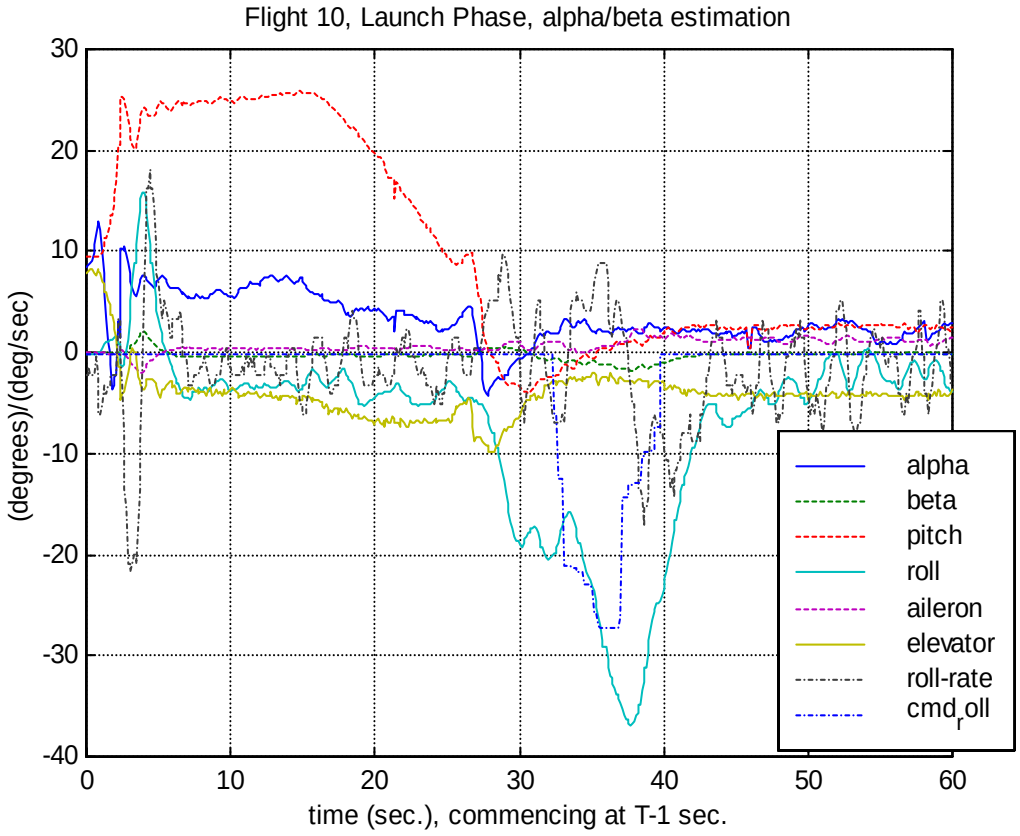
Flight 10, Launch Phase, alpha/beta estimation
alpha
beta
pitch
roll
aileron
elevator
roll-rate
cmd_roll
(degrees)/(deg/sec)
time (sec.), commencing at T-1 sec.
30
20
10
0
-10
-20
-30
-40
0
10
20
30
40
50
60

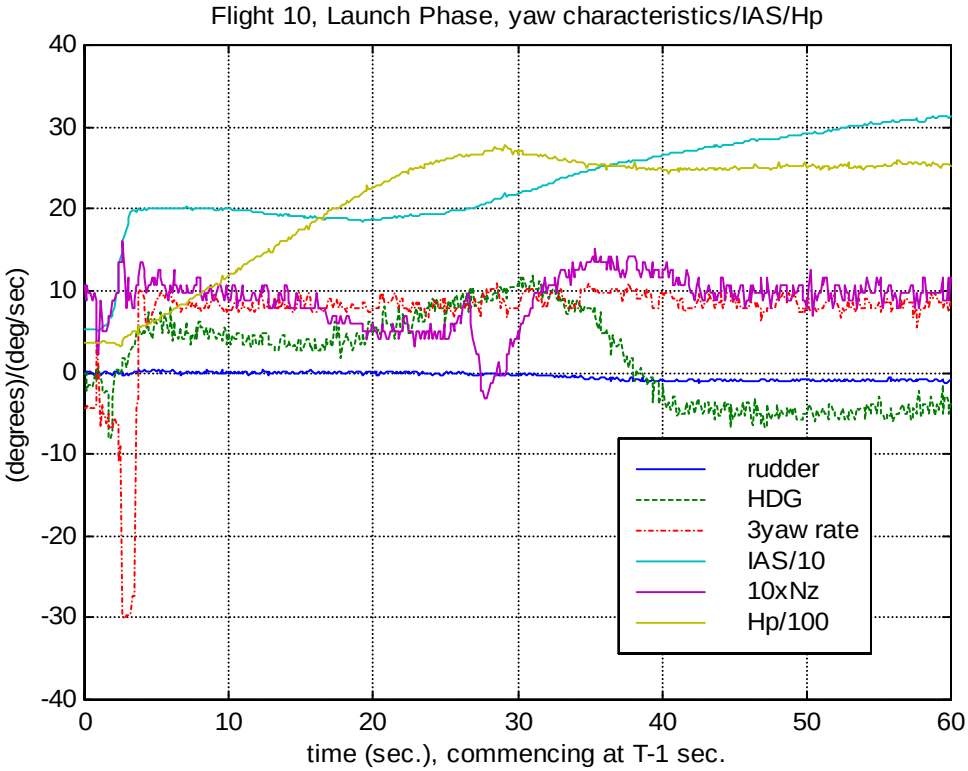

3.3.3.1 Peak launch incidence was 10.3°. At peak incidence, and approximately coincident with RATO-separation, a $-L_P<0$ roll occurred. The roll was arrested with DAP-commanded aileron deflection, and returned through null roll in an overdamped (i.e. non-overshooting) manner to a slight negative offset, which was, as before, maintained by aileron deflection. Therefore, a mild flow separation occurred through the pitch-up sequence. At the 'bunt', completing the pitch-down, an $-L_P<0$ roll occurred, evidence of significant lower-surface flow separation. The roll was arrested by DAP-commanded aileron, as incidence was near zero.

3.3.4 FQT 11:

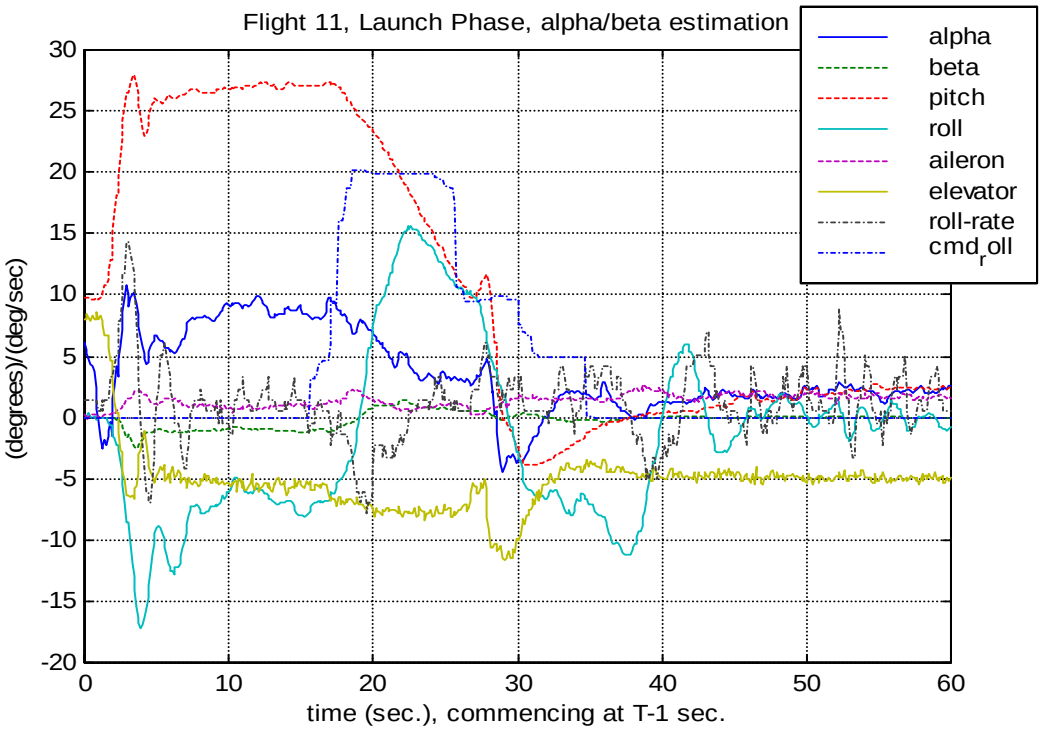

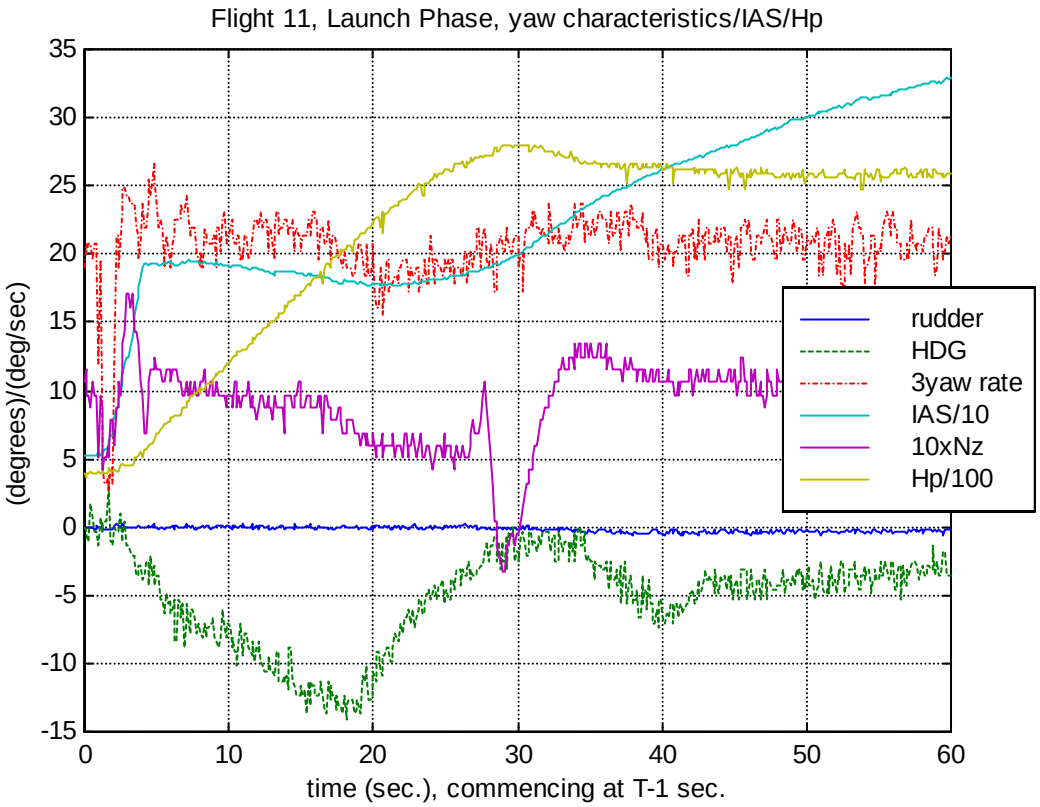

3.3.4.1 The launch pitch-up was similar to FQT 9 and 10; however, the initial roll direction was reversed, and the recovery from the roll more unstable. Once settled, the DAP maintained a roll-offset, rather than nulling the roll.

3.3.5 FQT 12:

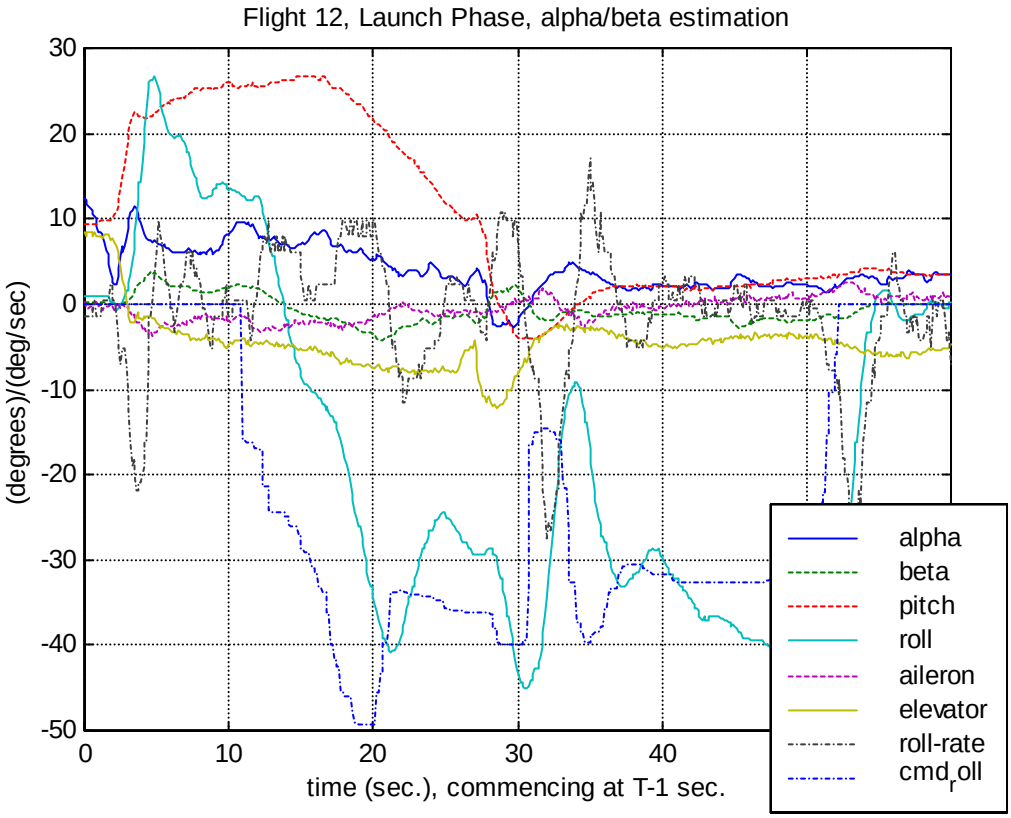

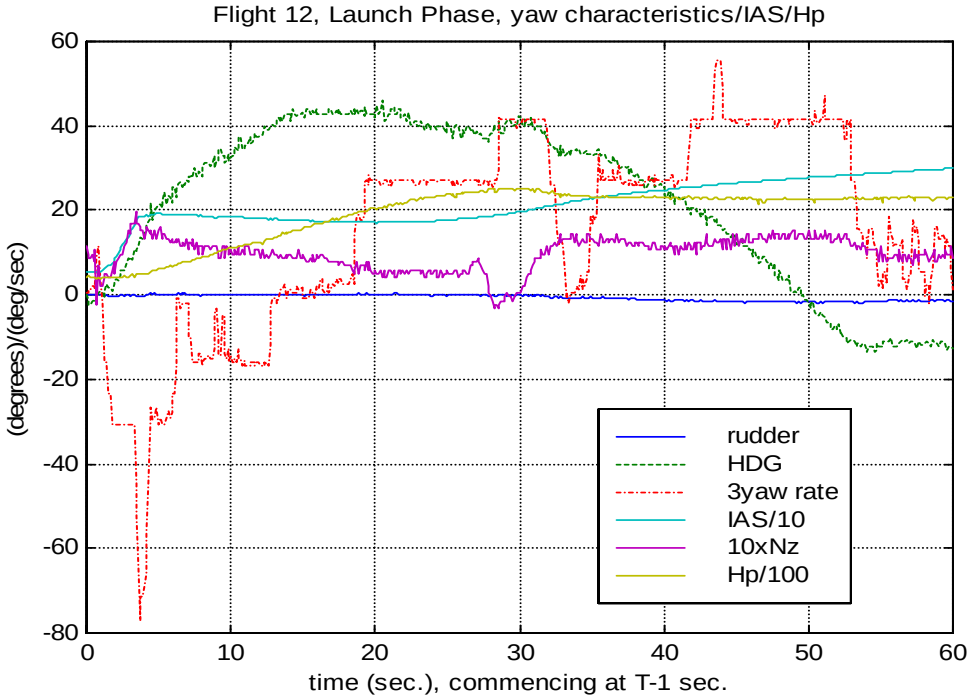

3.3.5.1 At launch pitch-up, a peak incidence of 11.5°, slightly greater than FQT 09, 10 and 11, but less than FQT 8, was achieved. Uncommanded roll onset was coincident with an incidence rise through approximately 7°. Roll-rate was in-phase with incidence. With reducing incidence (to 7°) and increasing DAP-commanded aileron, the roll was contained to 26.7°. The above characteristics were indicative of the occurrence of a substantially greater degree of flow separation. As previously, DAP-commanded aileron did not null the roll angle. At T+10, early CMD_roll inputs were made, presumably to limit the HDG excursion. At the pitch-over completion 'bunt', uncommanded roll occurred, as before.

3.3.6 FQT 13:

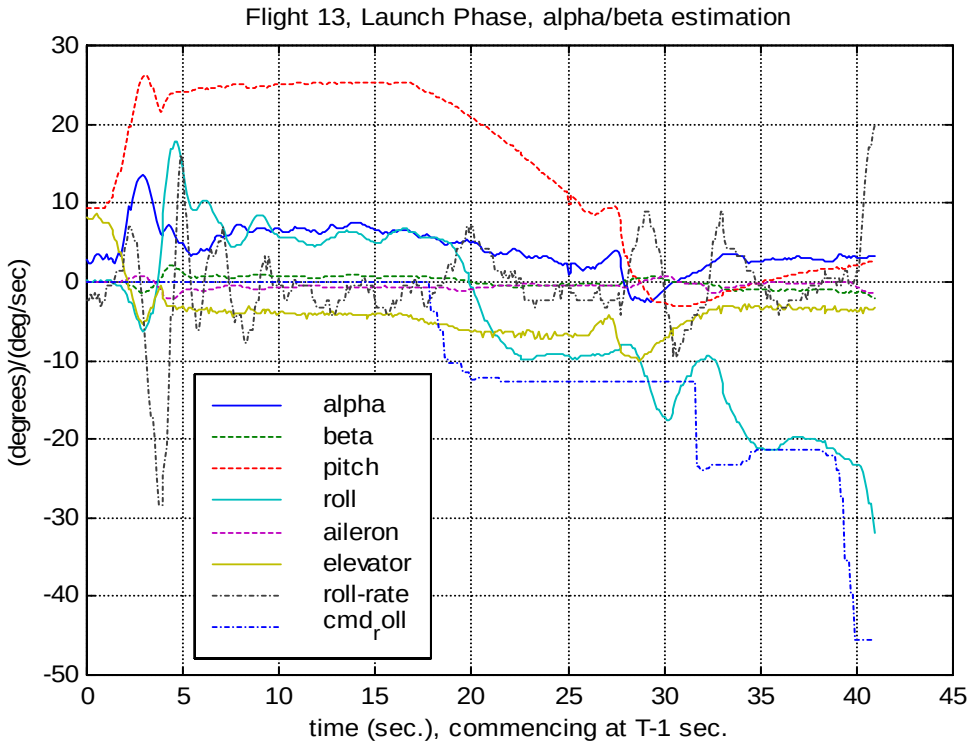

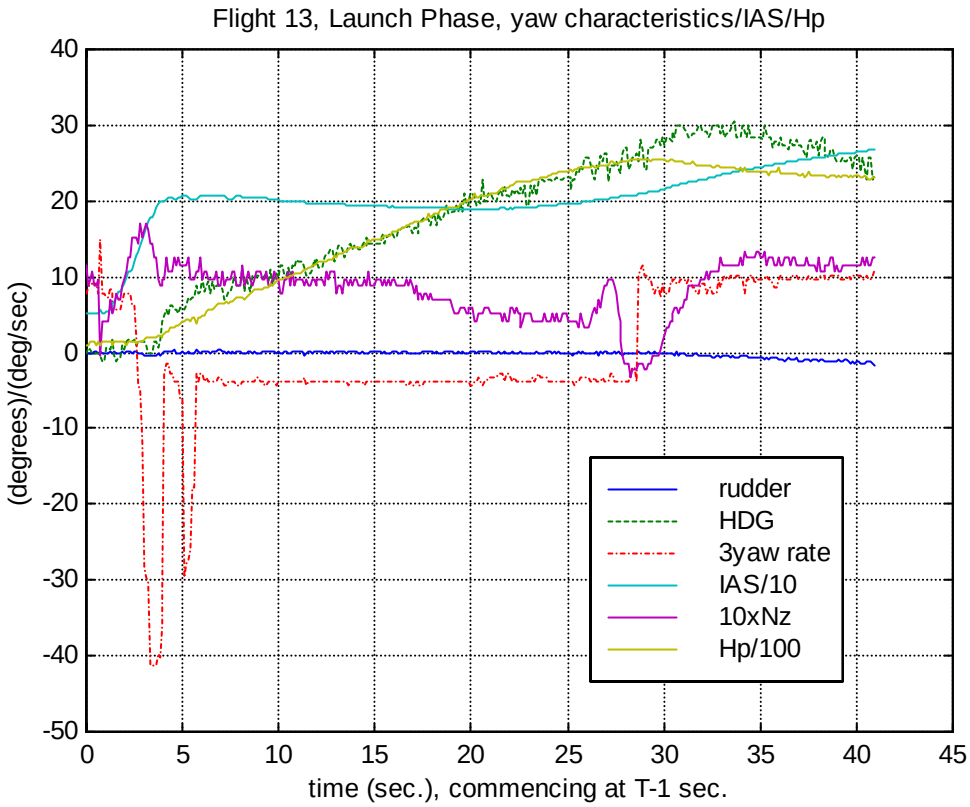

3.3.6.1 The roll behaviour is evidence of some mild flow separation occurring during the pitch-up, sufficient to reduce $-L_P$ to neutral/slightly negative and result in roll-overshoot upon DAP-correction. However, as before, the DAP did not command aileron to null the roll angle.

3.3.7 FQT 14:

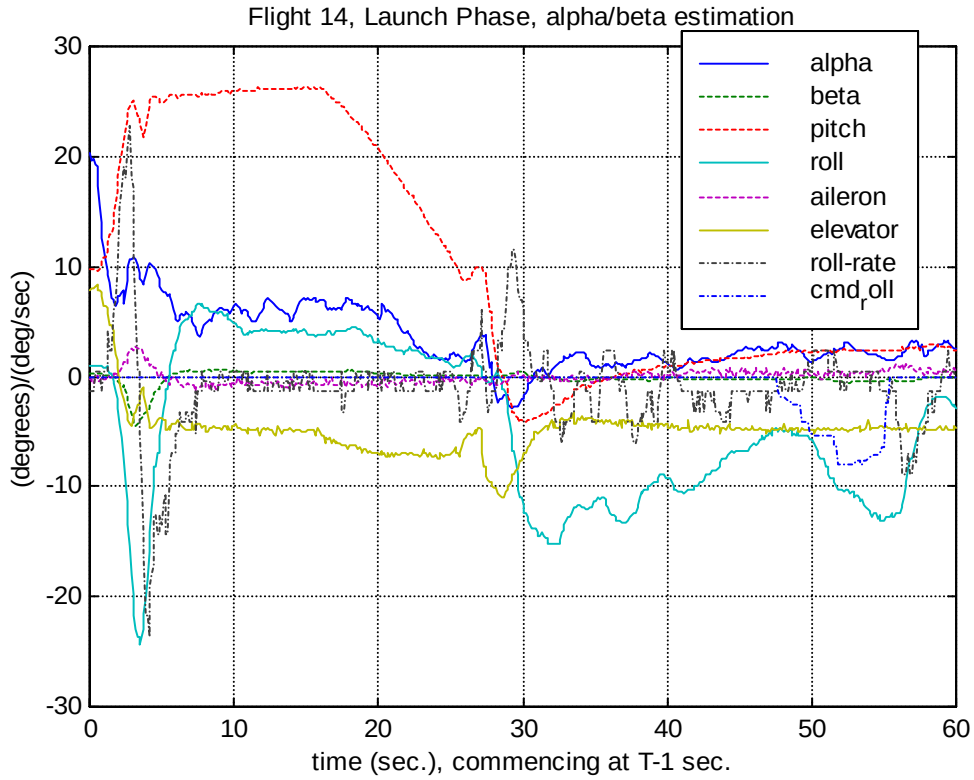

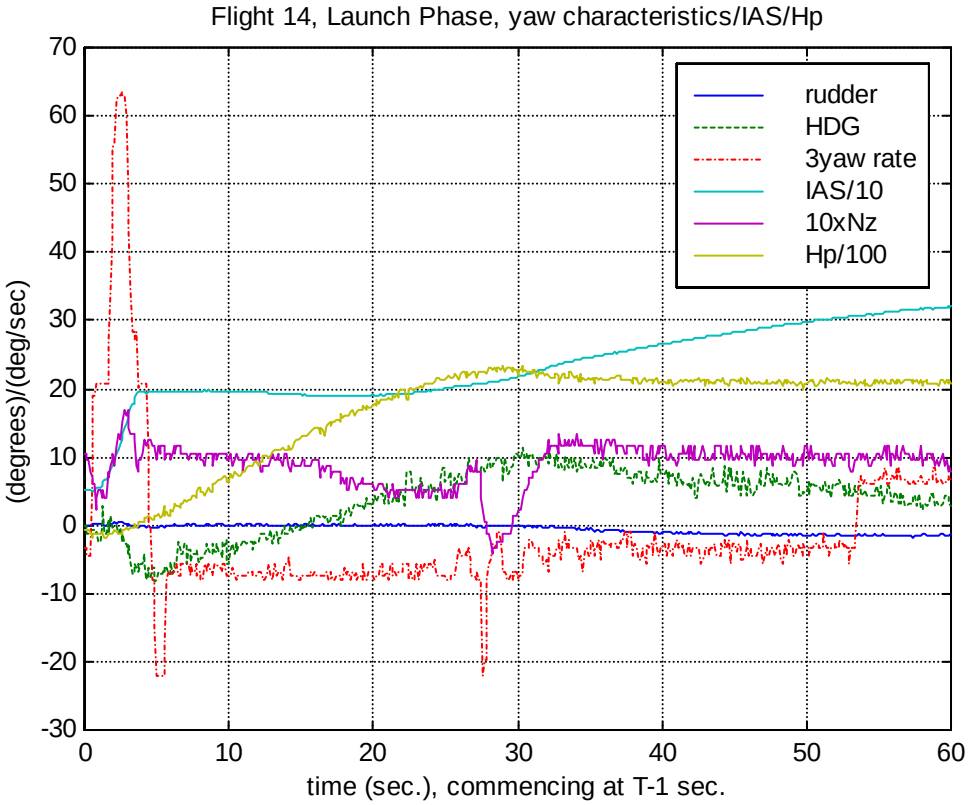

3.3.7.1 A sharp uncommanded roll excursion occurred at pitch-up. The roll was in-phase with the increasing incidence. Wind was calm. DAP-commanded aileron reversed the roll in an overdamped manner, indicative of a substantial degree of flow re-attachment. In spite of the overdamped return, however, a roll offset was maintained by the DAP, rather than commanding a roll null. At the pitch-down completion 'bunt', roll onset occurred at -2° incidence.

3.3.8 FQT 15:

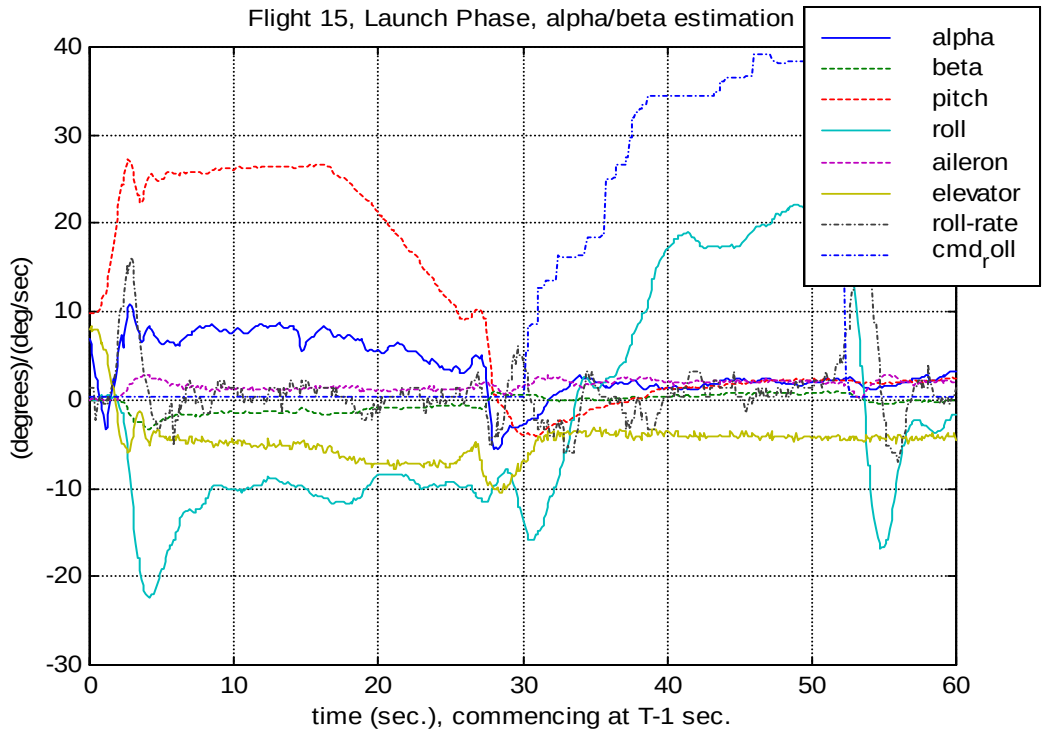

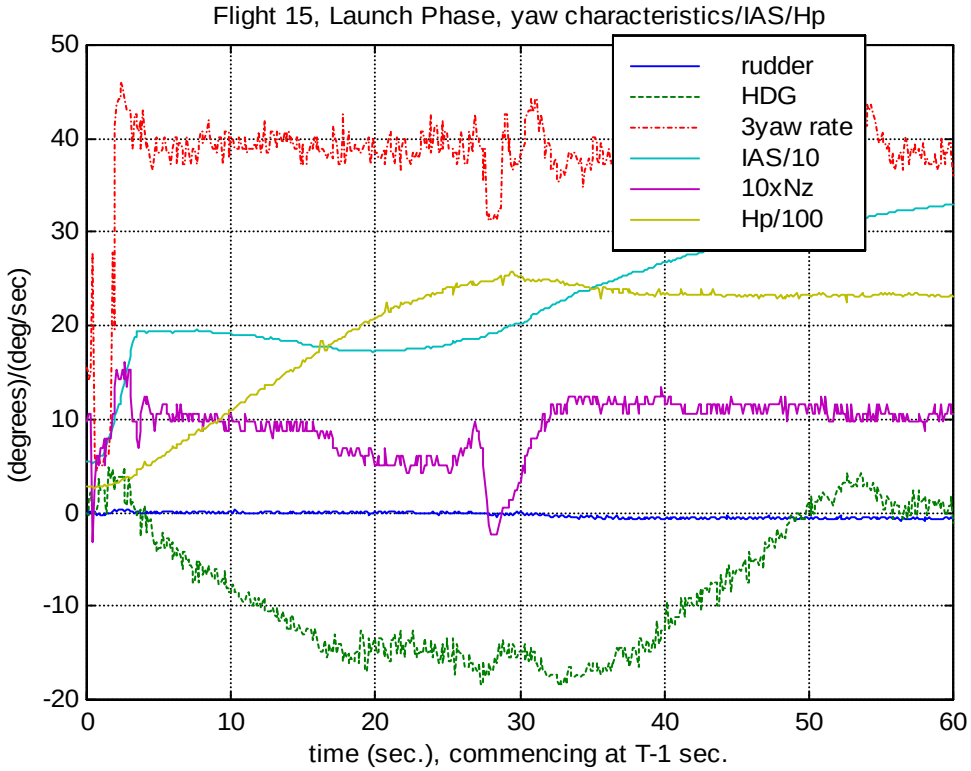

3.3.8.1 A right yaw is evidenced at launch-initiation. Wind was tail, at 4 knots. Uncommanded roll was initiated with the pitch-up, roll-rate was in-phase with incidence, indicative of substantial flow separation. DAP-commanded aileron arrested the roll, with incidence reducing to 7°. The roll angle was reduced in overdamped manner, indicative of a significant degree of flow re-attachment. A roll offset was maintained, rather than the roll angle returned to null.

3.3.9 FQT 16:

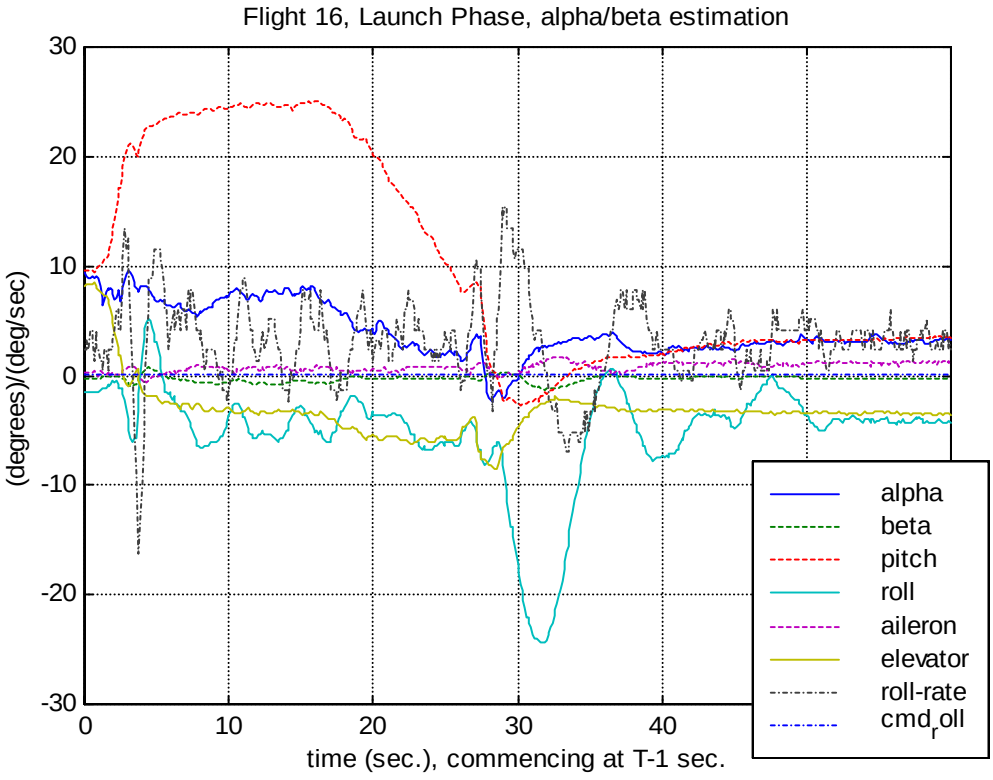

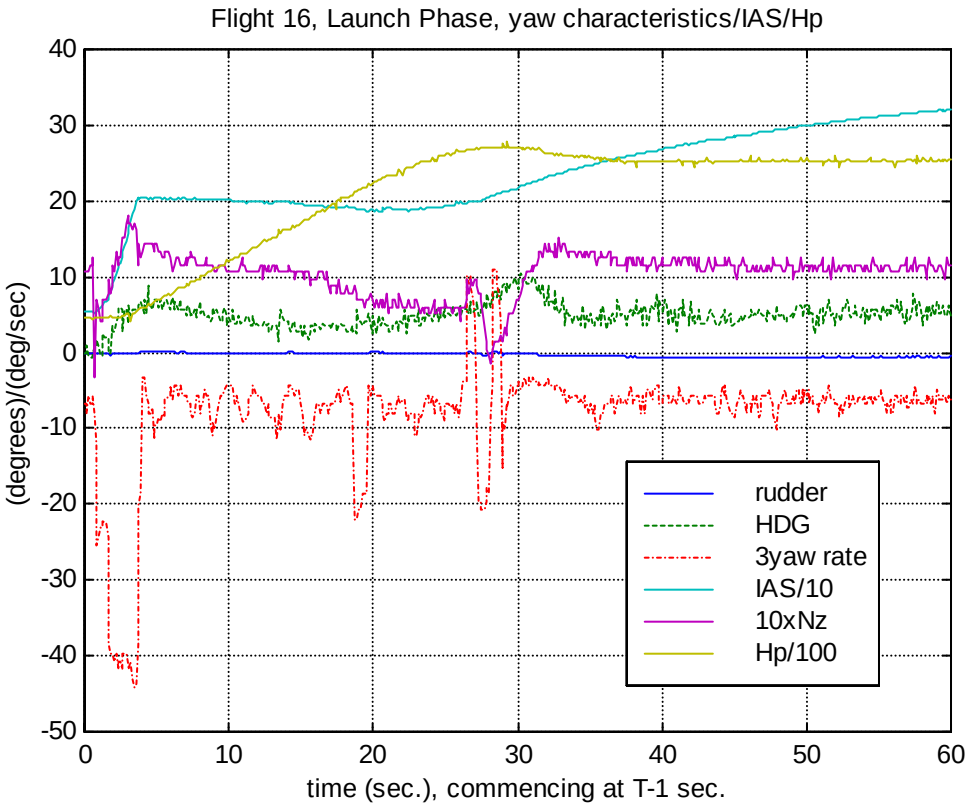

3.3.9.1 A right yaw occurred at RATO firing. However, there were negligible flow separation effects at pitch-up, evidenced in the above figures. A large uncommanded roll occurred at the 'bunt', $-L_P<0$ being evident of substantial flow separation.

3.3.10 FQT 17:

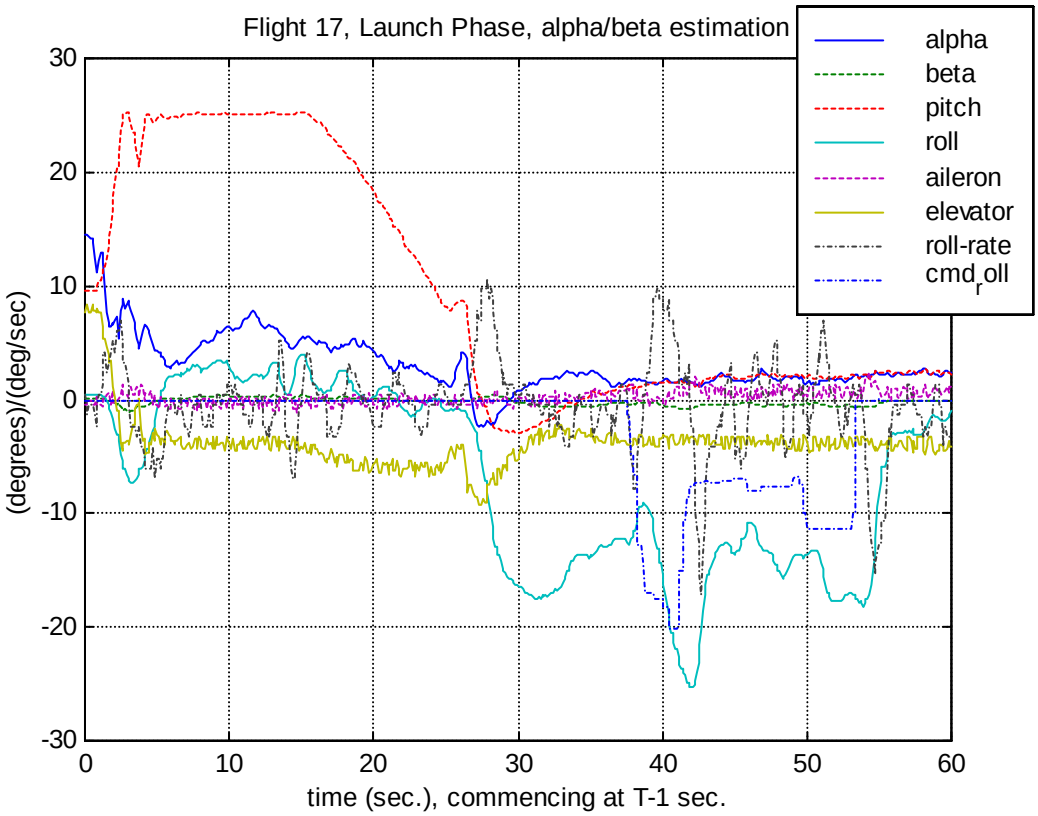

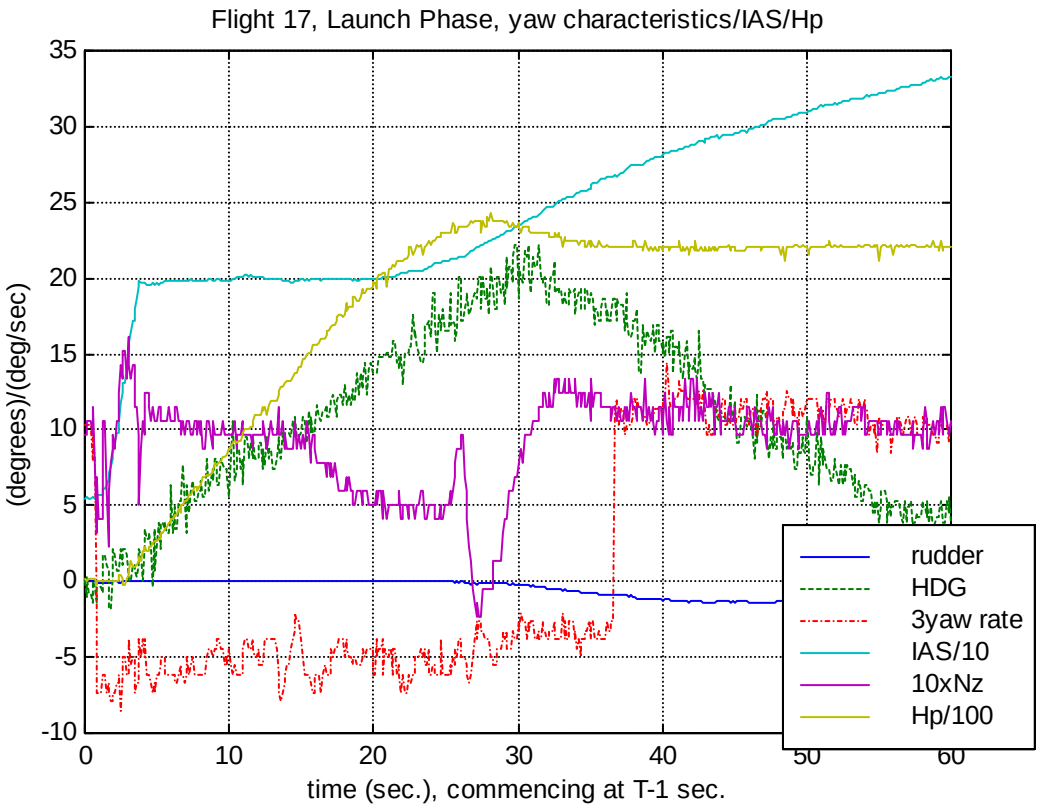

3.3.10.1 The aerodynamic and flight dynamic characteristics are very similar to FQT 16.

3.4 NIL stores

3.4.1 FQT 1:

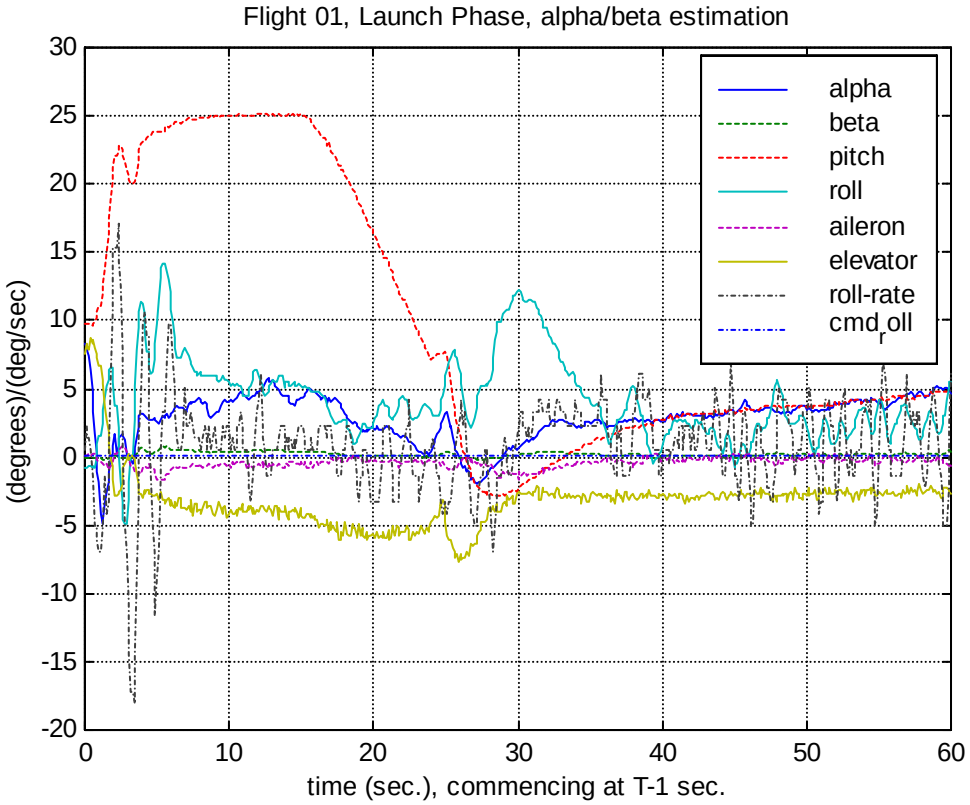

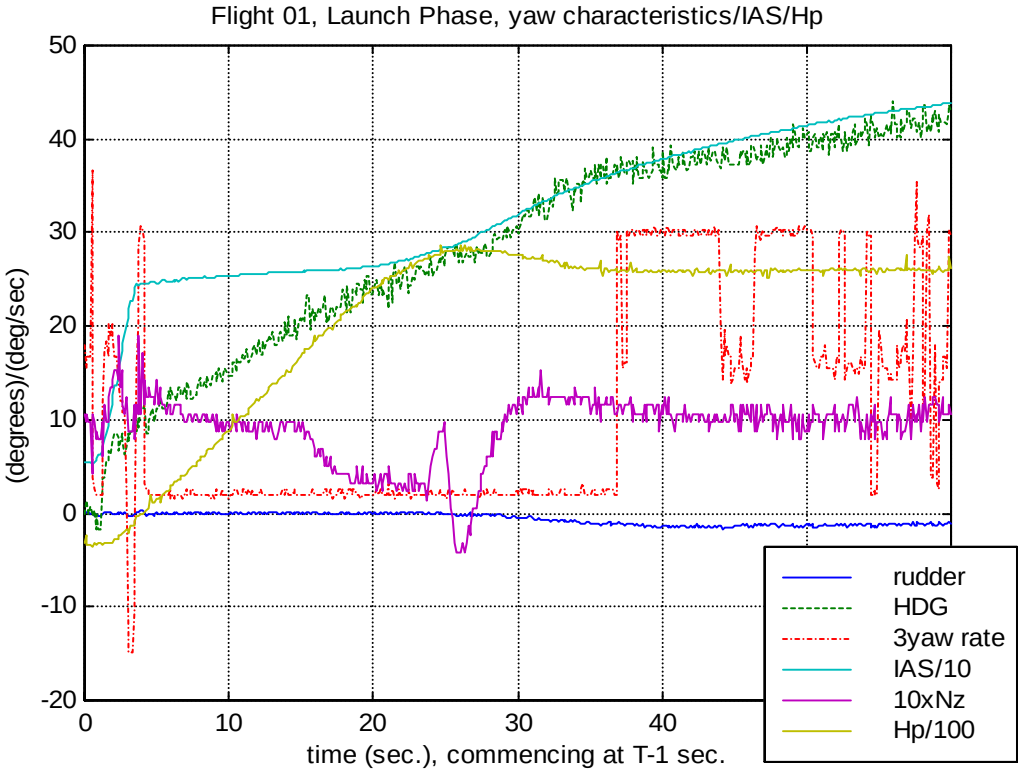

3.4.1.1 The launch is low incidence, a RATO-firing minimum of -4.9°, followed by an initial positive peak of 3.3° and a progressive rise to 5°. Mild roll instability occurred, no evidence of any significant flow separation, with the possible exception of the non-controllability of roll angle to the null value.

3.5 TPT-6A x 2 stores

3.5.1 FQT 02:

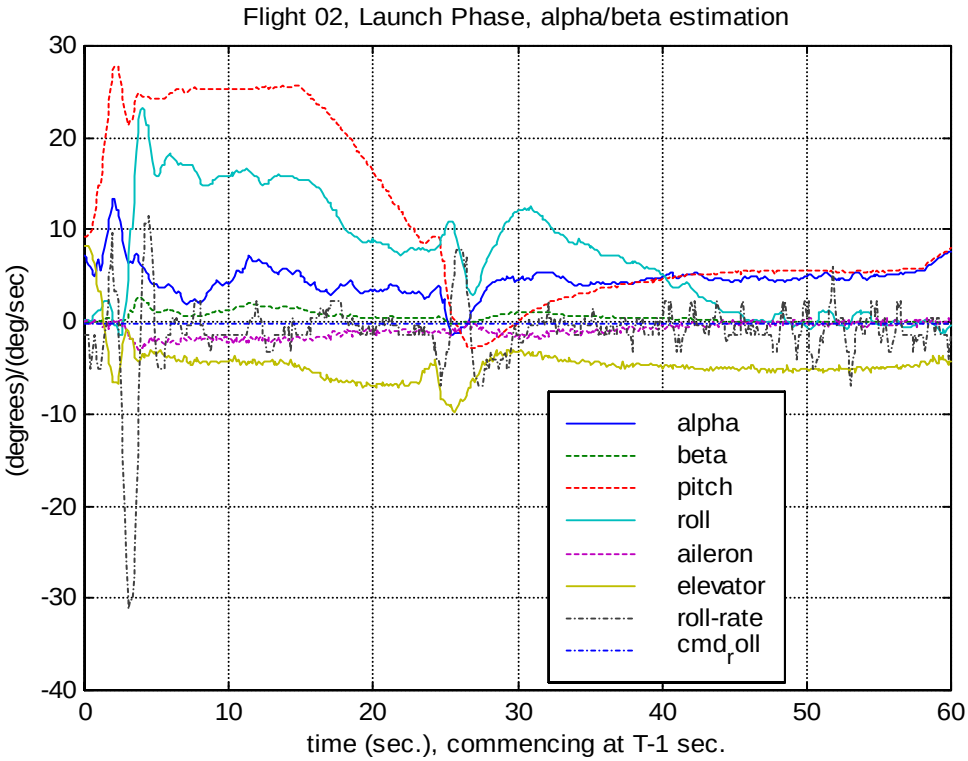

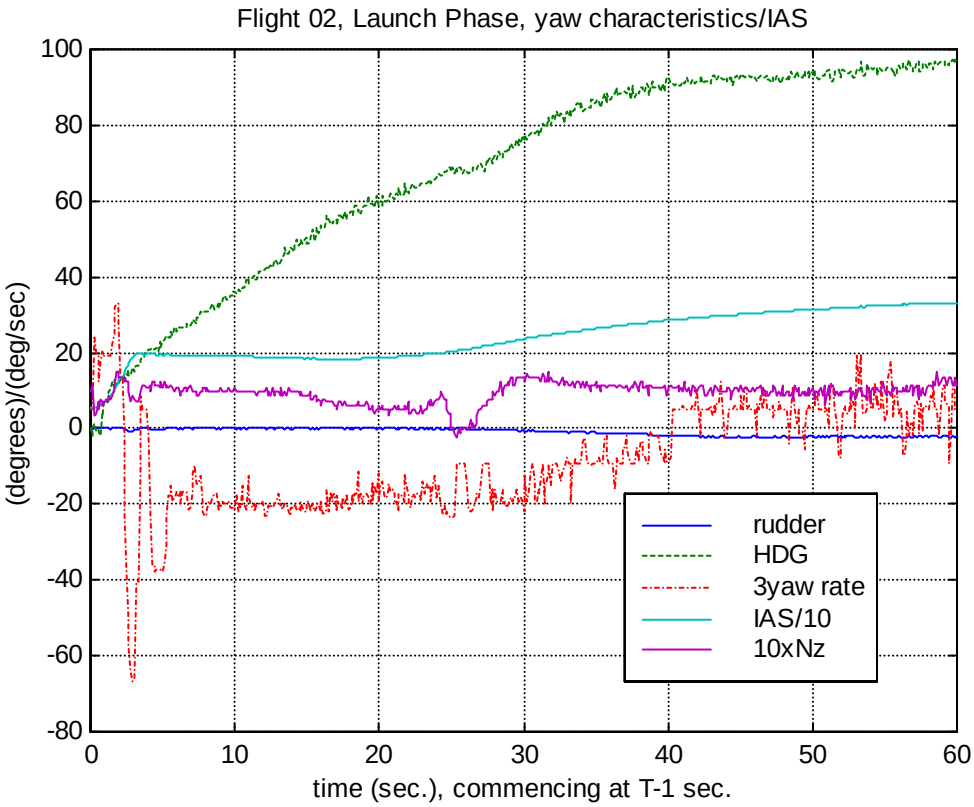

Following the peak pitch-up incidence of 11.9°, uncommanded right roll onset occurred. The roll was reversed by DAP-commanded aileron, with residual roll instability and the incidence reducing through 5°. This is evidence of significant flow separation.

3.5.2 FQT 05:

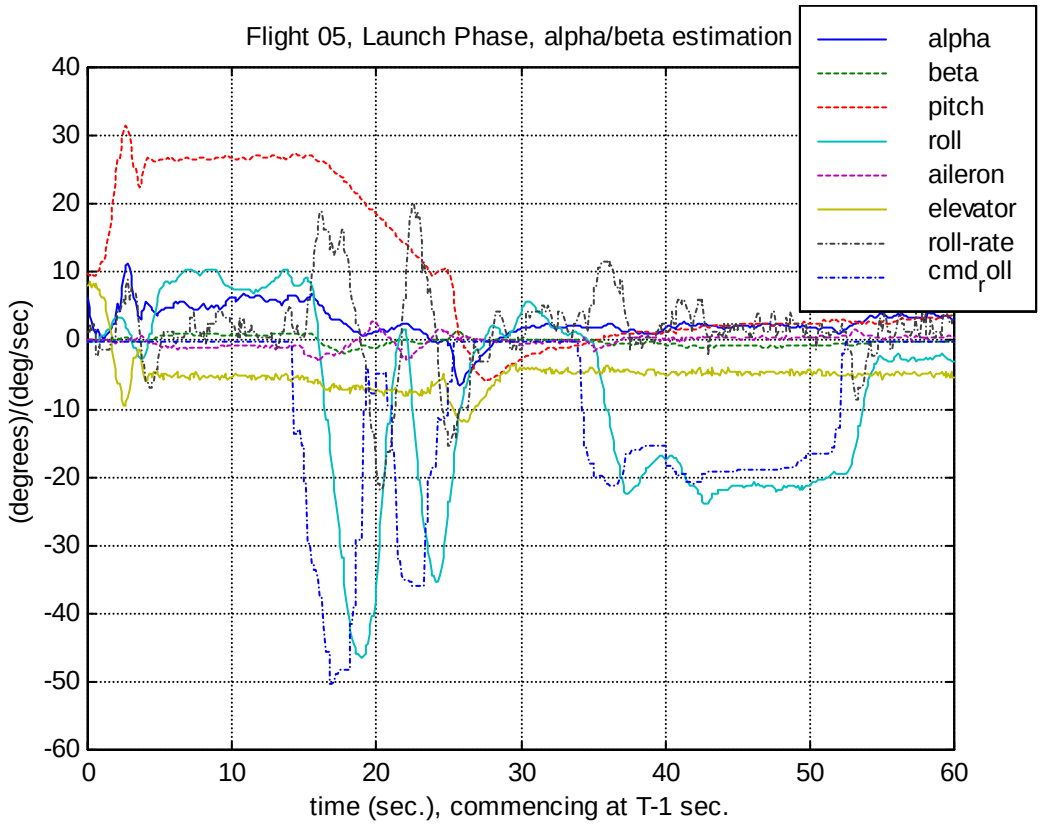

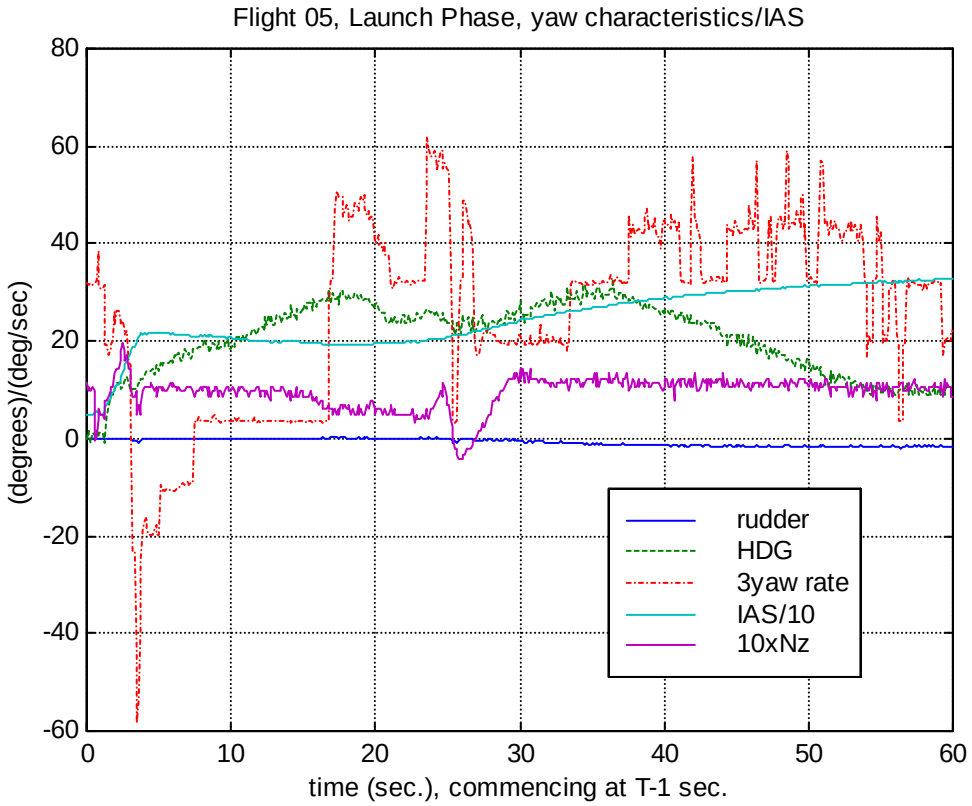

3.5.2.1 Pitch-up peak incidence was similar to that upon FQT 02. However, roll instability was negligible.

3.5.3 FQT 19:

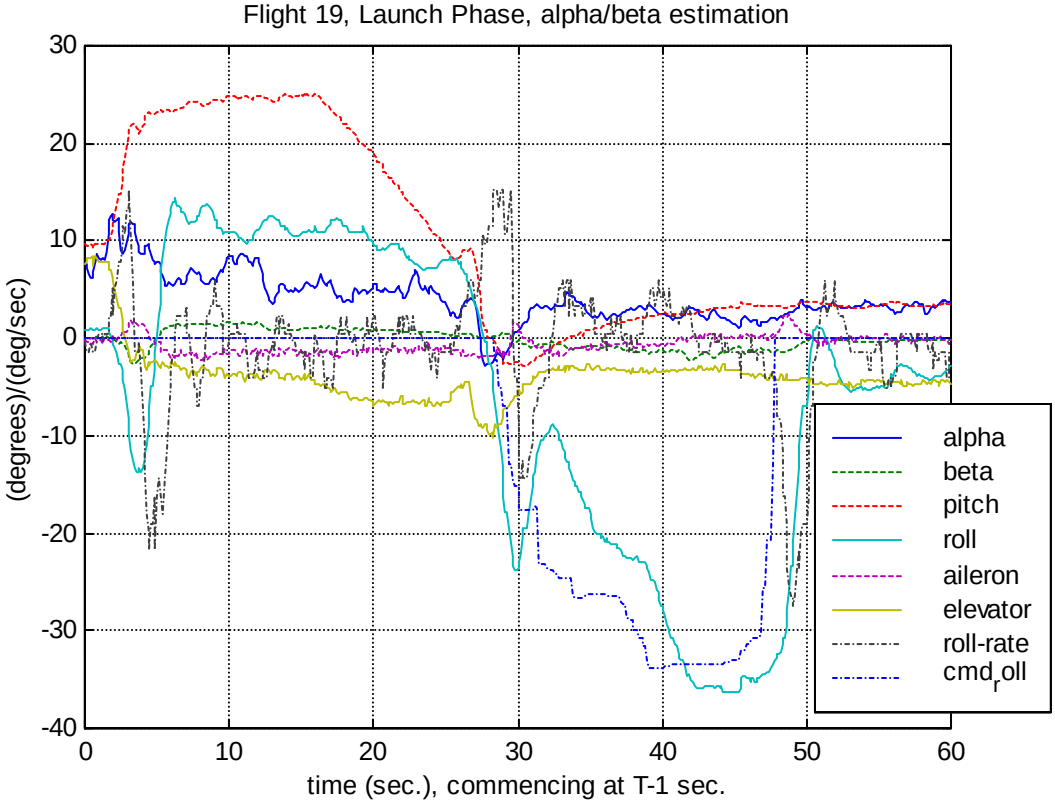

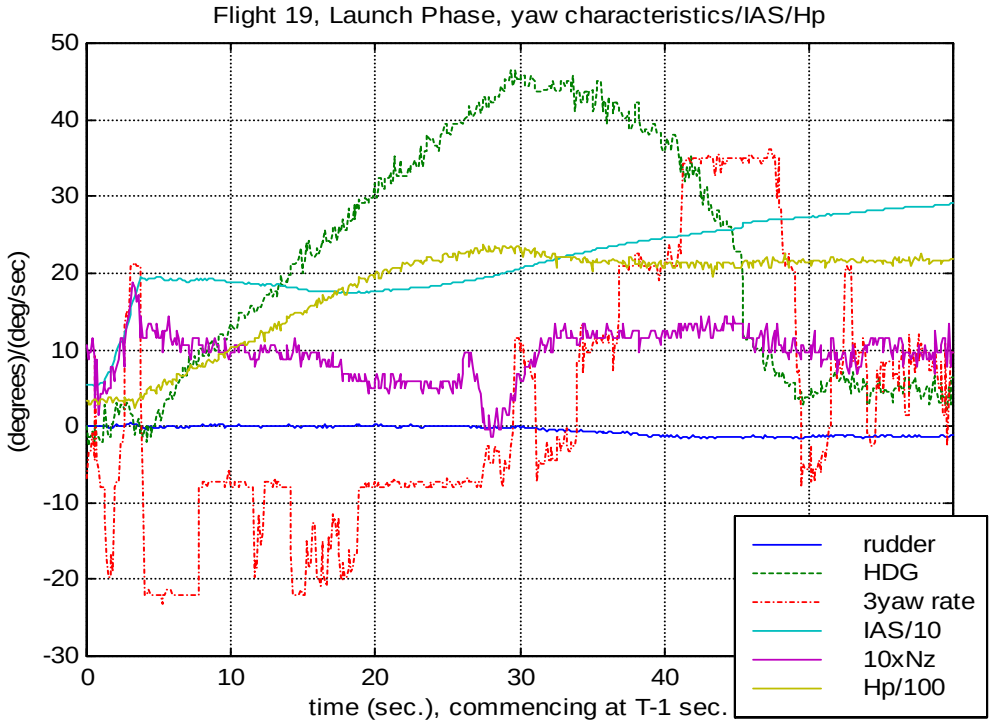

3.5.3.1 Peak pitch-up incidence is greater than that upon FQT 02 and 05, and uncommanded roll rate and amplitude are greater. DAP-commanded aileron arrested and reversed the roll, *albeit* with a substantial roll overshoot. Both characteristics are indicative of wing flow separation. Once stabilised, the DAP maintained a roll offset, rather than nulling the roll.

3.6 AWC18/APC4 stores

3.6.1 FQT 3:

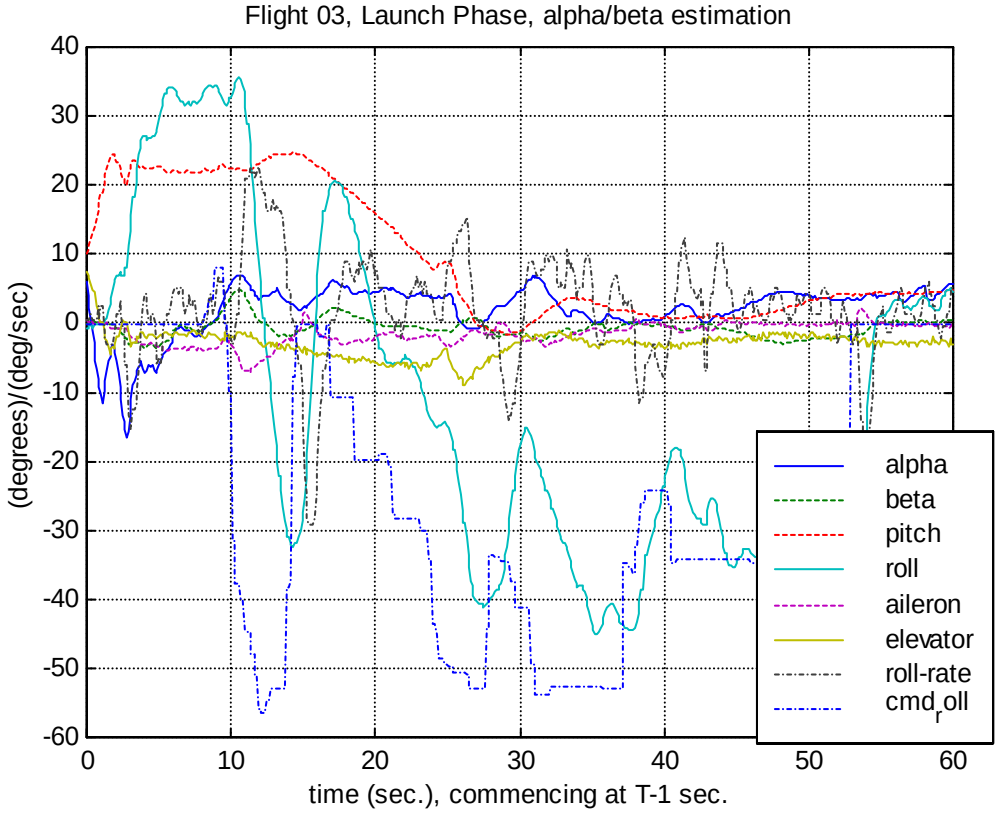

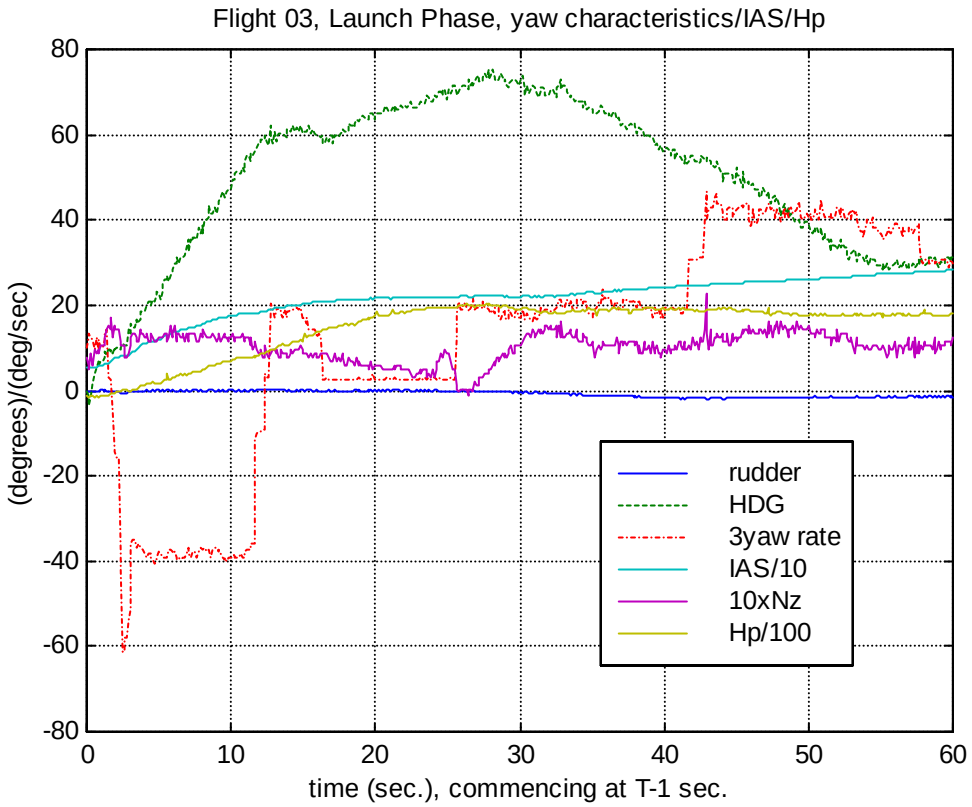

3.6.1.1 A large negative incidence quickly (-16.5°) built-up, following launch, and evidentially, substantial flow separation and uncommanded roll. Initially, the roll was partially arrested by DAP-commanded aileron. The roll was fully arrested, once the negative incidence had reduced in magnitude, below approximately -5°.

3.7 TPT6A(IR)/TRX17(RF) stores

3.7.1 FQT 6:

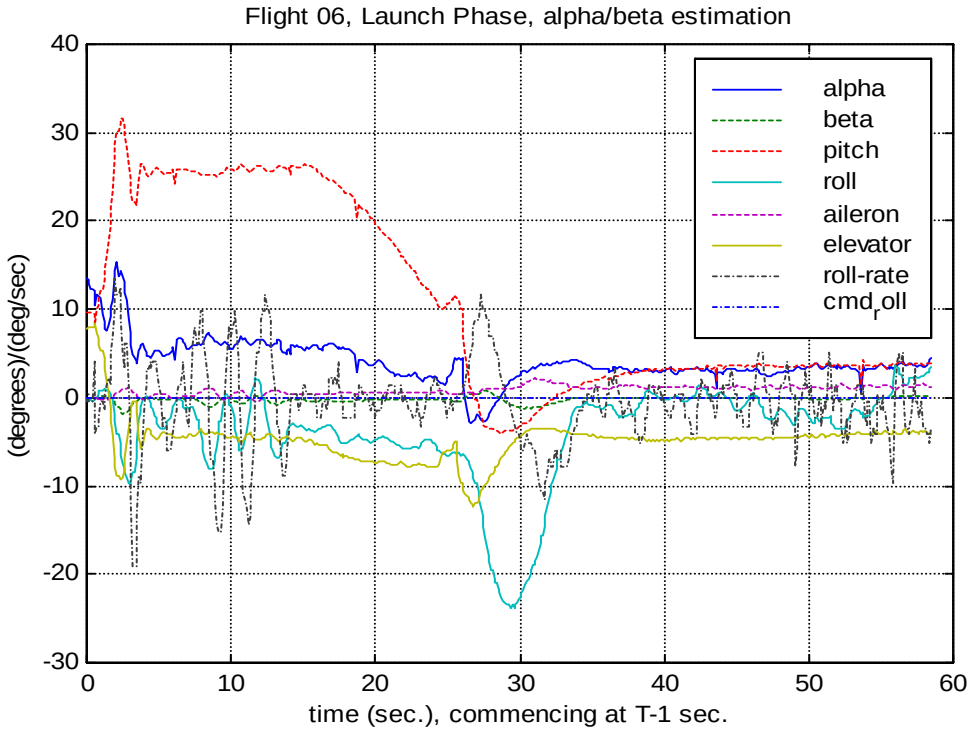

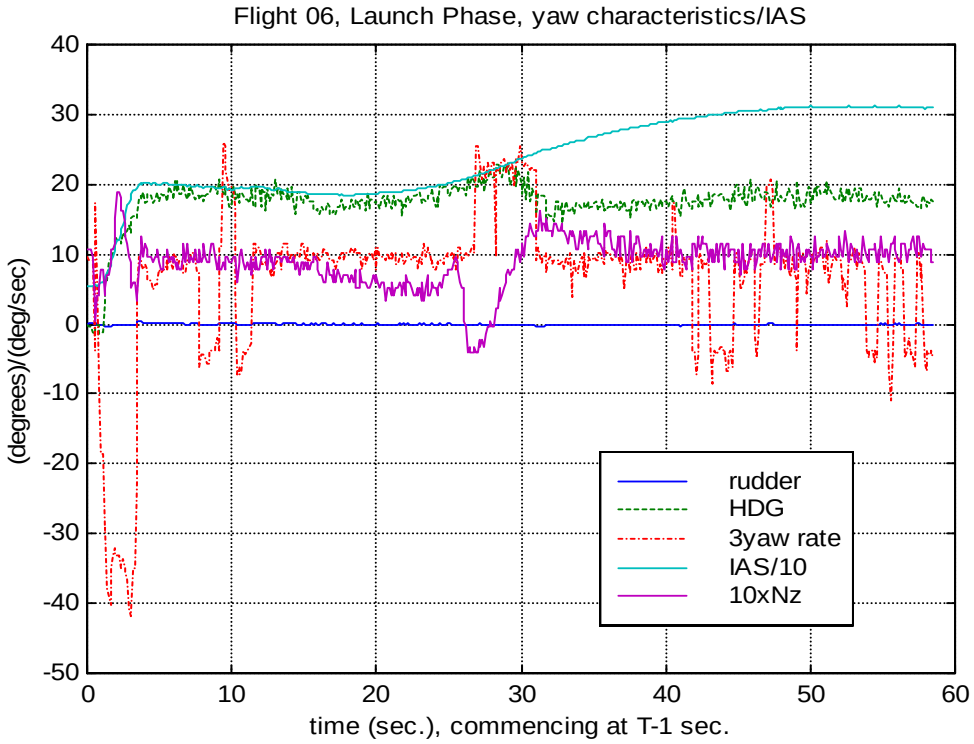

3.7.1.1 Upon launch, the aircraft encountered a starboard crosswind, which resulted in a starboard yaw, and a dutch roll-induced rolling motion. Although incidence peaked at 15.3°, there is no evidence of significant flow separation. The DAP scheduled 'high-gain' aileron inputs. Resultant rolling motion was of a neutrally-damped dutch roll-type of motion. When stabilised, a slightly divergent left roll was maintained, rather than controlled to a null roll angle. At the 'bunt', a separated flow-induced left roll to -24° occurred.

3.8 TRX17_2LENS x 2 stores

3.8.1 FQT 18:

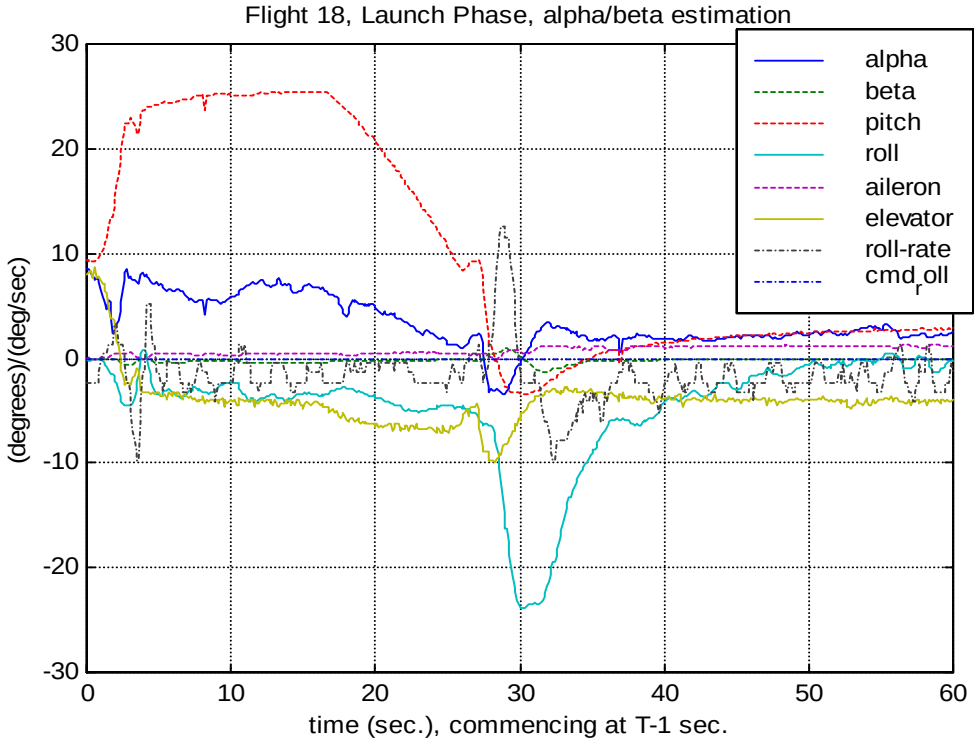

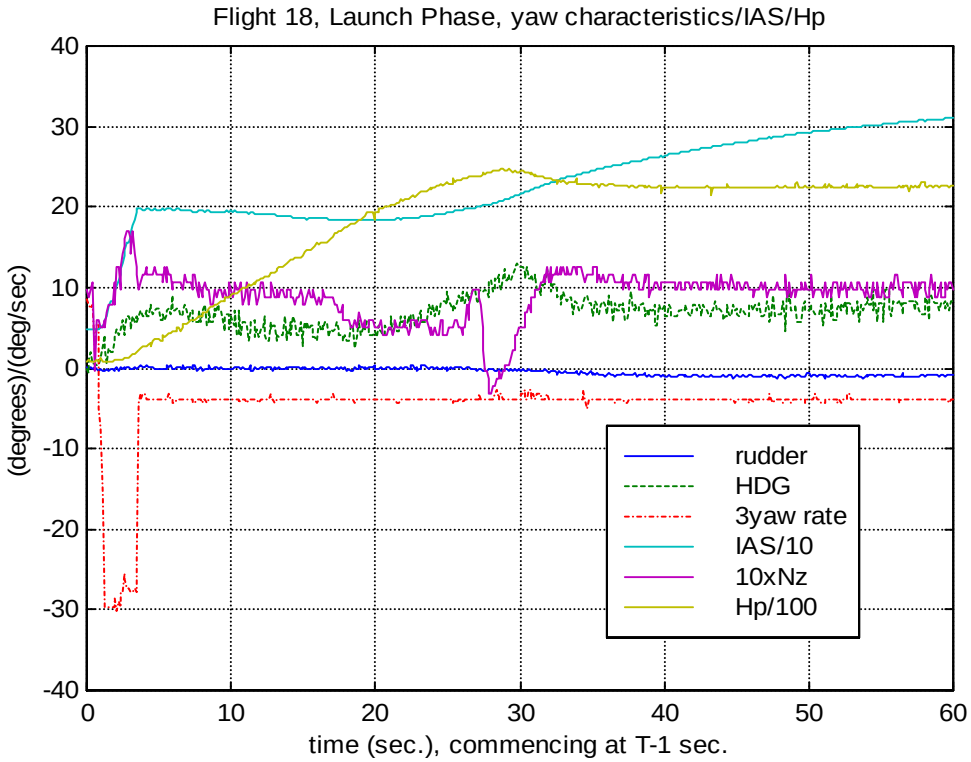

3.8.1.1 Negligible roll instability occurred during the initial launch phases. As upon FQT 6, at the pitch-down completion 'bunt', substantial uncommanded rolling motion occurred. The roll was not arrested by DAP-commanded aileron, until the incidence magnitude reduced to -1°.

3.9 WINGTIP&AWC x 2 stores

3.9.1 FQT 20:

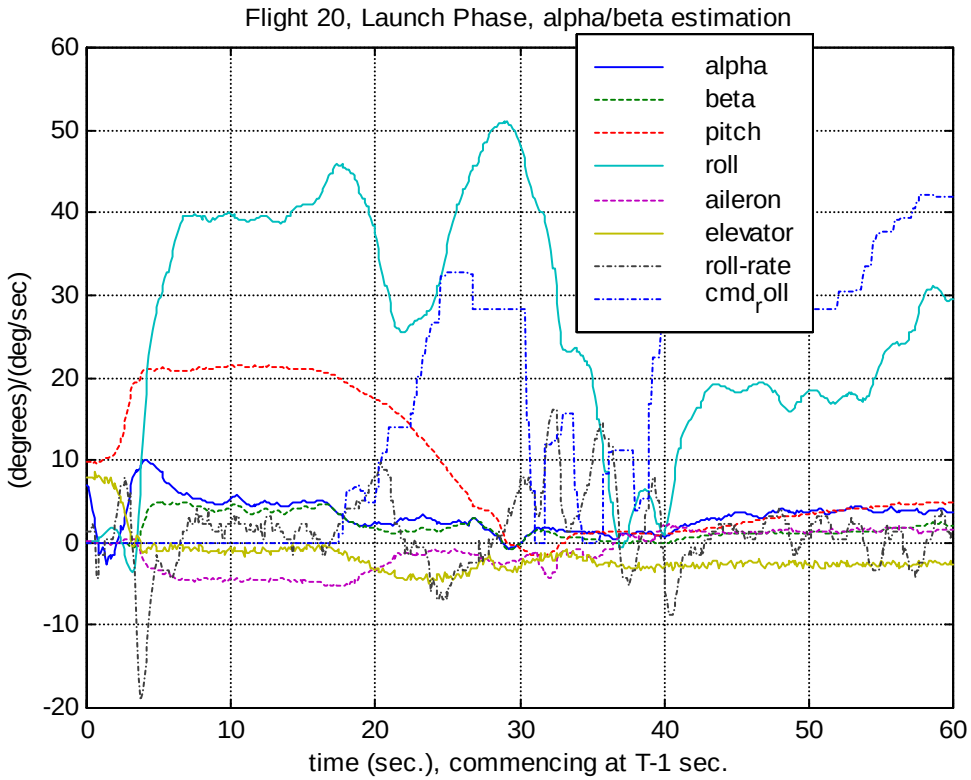

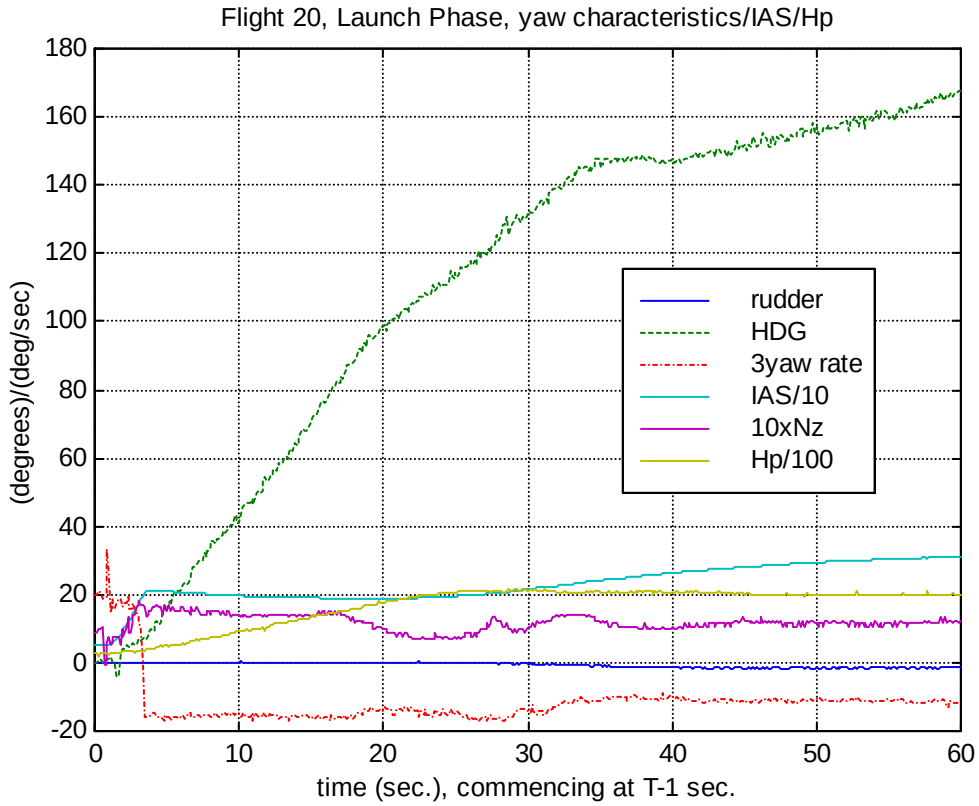

3.9.1.1 Large-scale wing flow separation is evidenced, during the pitch-up, with uncommanded roll onset occurring at an approximate incidence of 8°. DAP-commanded aileron arrests the rolling motion, at a roll displacement of 39°, with the incidence reducing to 6.5°, at this point. The incidence reduces further, to 5° at T+9 seconds. At T+13.5, there is a very slight increase in incidence and aileron deflection (the latter, from -4.5° to -4.8°). The result was a mild combined loss in roll damping and aileron effect, so that the roll displacement increased further. Greater losses in L_P and $L_{\delta a}$ occurred at T+15.3, as a result of a further increase in aileron deflection, from -4.8° to -5.3°.

3.9.1.2 Thus, there is no lateral control margin in this condition, indicative of a substantial amount of residual separated-flow, particularly over the aileron upper surfaces. At time T+16.7, with incidence reducing through 4°, positive roll damping and aileron effect returned, resulting in a reduction in roll displacement. This is indicative of substantial flow re-attachment occurring at this point. Subsequently, a positive roll occurred at T+22, whereat the aileron deflection was approximately -1.5°. However, this occurrence could be due to the commanded aileron being insufficient to balance L_β, due to the higher residual sideslip angle at this point.

3.9.1.3 In other words, the separated-flow hysteresis region extended, in this case, over an incidence range of 8° to 10°, thence to 4°. The extent of separated flow can be appreciated by the size of the hysteresis effect.

3.10 Summary

3.10.1 The flight mechanical and dynamic characteristics, for all flights, are summarised in Table 1, wherein they are grouped by configuration, and cover the pitch-up initial launch phase, the 'bunt' at the completion of the pitch-down manoeuvre, and the quasi-steady roll-offset segment of the launch phase.

Table 1 - Summary of Flight Mechanical/Dynamic Characteristics of FQT Launches

FQT	Peak pitch-up alpha (deg)	Pitch-up response roll rate (deg/sec)	Pitch-up response roll angle (deg)	Roll return	Quasi-steady Roll offset			Pitch-over 'Bunt' peak negative alpha	Pitch-over 'Bunt' response roll rate	Pitch-over 'bunt' response roll	30sec overall heading change
					alpha	aileron	roll				
TPT17RF/TRX17DUMMY											
08	13	-31	-23.5	Undamped, $-L_P<0$	6.0	-0.5	2.3	-4.2	-12	-22	32
09	10.9	Init. yaw	12.5	Undamped, $-L_P<0$	5.6	1.5	-12.5	-6.8	-8.5	-25.1	-3 (max 10)
10	10.3	21.3	15.9	Damped, $-L_P>0$	5.2	0.3	-2.7	-4.2	-10	-19.3	10
11	10.9	-14.2	17.1	Neutral	8.1	1.0	-8.0	CMD	N/a	N/a	-2 (max -12)
12	11.5	21.5	26.7	Damped, $-L_P>0$	7.1	-2.0	16.2	CMD	N/a	N/a	40 (max 44)
13	13.6	27	17.7	Neutral	6.2	-0.8	7.1	CMD	N/a	N/a	28
14	10.9	-23	24.4	Damped, $-L_P>0$	6.0	-0.7	4.7	-2.9	-11.5	-15.2	10
15	10.9	-16	-22.4	Damped, $-L_P>0$	7.6	1.4	-11.2	-5.6	6	-15.9	-16
16	9.7	-13	-6.2	Undamped, $-L_P<0$	7.3	0.7	-4.9	-2.3	-15	-24.4	10
17	8.8	-6.7	-7.3	Damped, $-L_P>0$	5.3	-0.2	2.1	-2.5	-10	-17.5	21
NIL											
01	-4.9 (neg)	6/-17/18	6.7	Undamped, $-L_P<0$, $L_{\delta a}<0$	4.3	-0.5	5.4	-2	7	12	30
TPT-6A x 2											
02	11.9	31	23.2	Lightly damped, $-L_P>0$	4.4	-1.9	15.9	-1.5	-8	-8	76
05	11.2	-8	-3.5	Lightly damped, $-L_P>0$	5.6	-0.9	8.7	CMD	N/a	N/a	26 (max 30)
19	12.8	-15/20	-13.8	Undamped, $-L_P<0$	5.7	-1.4	11.1	CMD	N/a	N/a	46
AWC18/APC4											
03	-16.5 (neg)	16	27	Undamped, $-L_P<0$	0.7	-3.5	33	CMD	N/a	N/a	73
TPT6A(IR)/TRX17(RF)											
06	15.3	-15/19	10	Undamped, $-L_P<0$	5.9	0.3	-3.2	-2.9	-11	-24	22
TRX17(2LENS) x 2											
18	8.5	4	-4	Neutral	6.1	0.4	-3.3	-3.4	-12.5	-23.8	12
WINGTIP&AWC x 2											
20	10	18.5	39	Damped, $-L_P>0$, $L_{\delta a}<0$	4.9	-4.5	40	Under CMD	N/a	N/a	132

3.11 Flight Mechanical/Dynamic Characteristics

3.11.1 General

3.11.1.1 Relevant to system safety analysis, there are a number of flight mechanical/dynamic characteristics during the launch phase of flight, which are of concern:

a. Variability of pitch-up incidence;

b. Extent and variability of wing flow separation and resultant loss of roll stability;

c. Magnitude of roll-offset, maintained by the DAP during the quasi-steady climb;

d. Variability of elevator deflection control by the DAP, during pitch-up and pitch-down;

e. Extent of wing flow separation and loss of roll stability, during the 'bunt' at the completion of the pitch-down segment; and

f. Anomalous parameter values.

3.11.2 Variability of pitch-up incidence

3.11.2.1 Two aircraft configurations have been the subject of multiple launches: TPT17RF/TRX17DUMMY, ten launches, and TPT-6A x 2, three launches. For both configurations, launch incidence and flight dynamic response envelopes differ significantly between individual launches; for example, of ten launches the TPT17RF/TRX17DUMMY configuration has a mean peak incidence of 11.1° and standard deviation 1.4°. In part, the variability could be attributable to launch wind/atmospheric conditions. It could also be due to variations amongst individual components of, nominally the same build standard (a production tolerance attribution).

3.11.3 Wing flow separation on pitch-up

3.11.3.1 Most launches exhibit evidence of wing-flow separation, to some extent, during the pitch-up segment of the launch phase. The typical manifestation was an uncommanded roll (i.e. loss of roll stability, manifested by negative roll damping, $-L_P$). In all cases, the DAP commanded recovery aileron, and except for FQT 01 and 20, aileron effect, or roll power, $L_{\delta a}$ was positive (for FQT 01, clean wing, and 20, WINGTIP&AWC x 2, the application of roll resulted in an increase in roll displacement, i.e. both $-L_P<0$ and $L_{\delta a}<0$). Typically, incidence was reducing at this point. Roll damping, however, often remained neutral or negative, resulting in overshooting roll-return characteristics. For all launches, after six roll cycles at most (depending upon the extent of flow separation, the DAP had managed to command quasi-steady roll angles); however, the roll angles were offset from wings-level (the 'null' roll position) to varying degrees.

3.11.3.2 As a response to separated wing-flow, it can be expected that the magnitude of the roll excursion, either roll rate or displacement, would be related to the peak pitch-up incidence. For example, for the TPT17RF/TRX17DUMMY configuration, both left and right roll breaks occurred. Roll-break displacements and roll rates, and the moduli of both, have been correlated against peak incidence values, in the following figures.

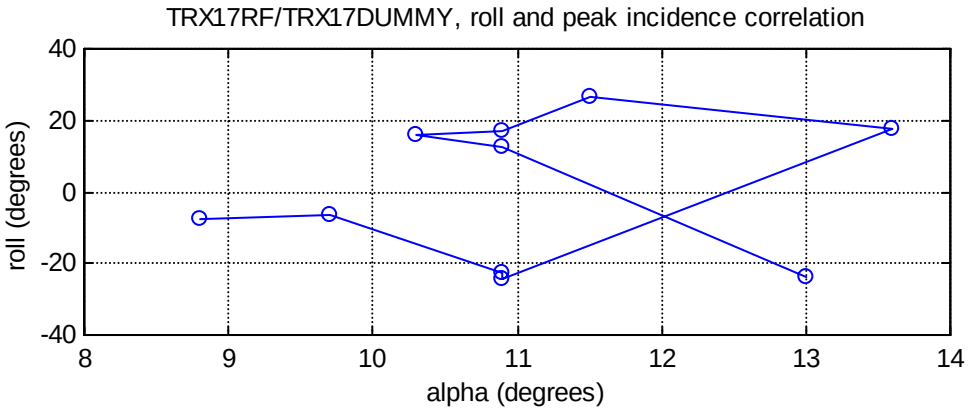

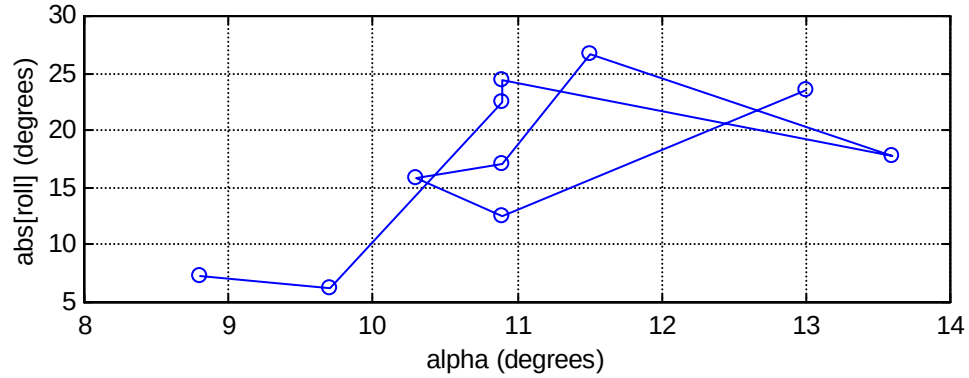

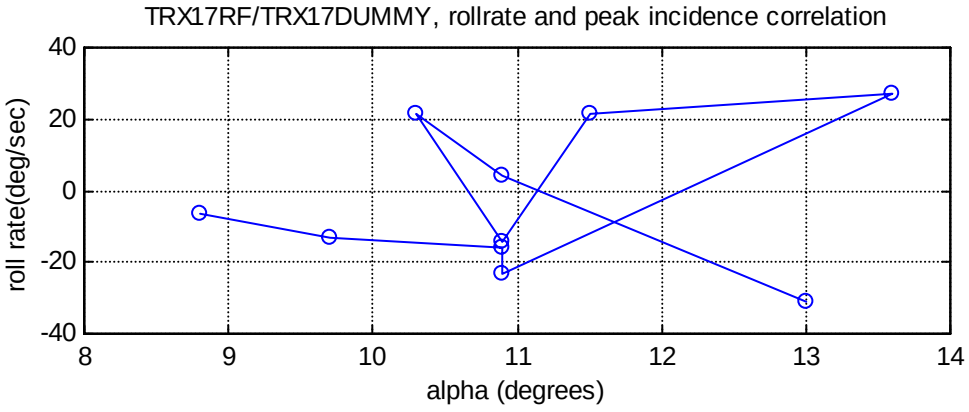

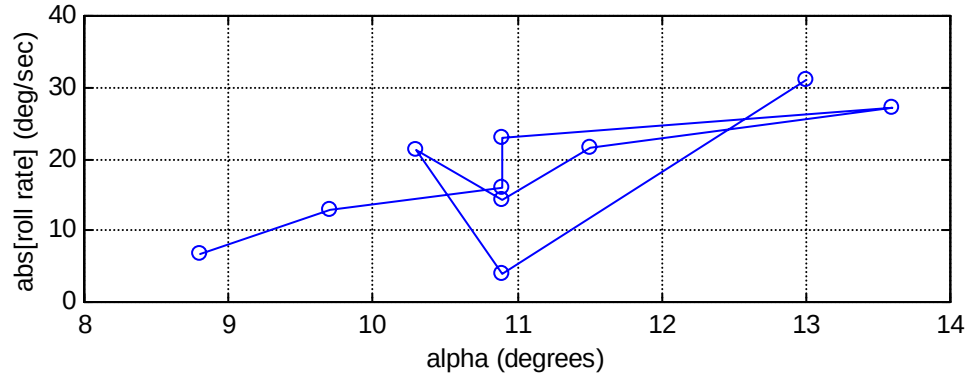

3.11.3.3 The above figures show that roll-break direction was random and that correlations of the moduli of both roll rates and roll displacements with peak incidence were reasonable. Given that the roll displacement was typically affected by the rate/magnitude of corrective aileron displacement that the DAP applied, it can be expected that the better correlation would be obtained for roll rate. As seen above, this is indeed the case. Furthermore, the modulus[roll rate]

and modulus[roll angle] correlations indicate that, upon extrapolation, negligible rolling motion would occur for peak incidence values no greater than 8°.

3.11.3.4 On FQT 18, the final flight manoeuvres consisted of a transient 6g steep turn and a level deceleration to manual drogue deployment. Analysis of the level deceleration indicates that an aerodynamic stall occurred, prior to drogue deployment. The stall was characterised by the simultaneous occurrence of an uncommanded rolling motion and an uncommanded incidence/g break.

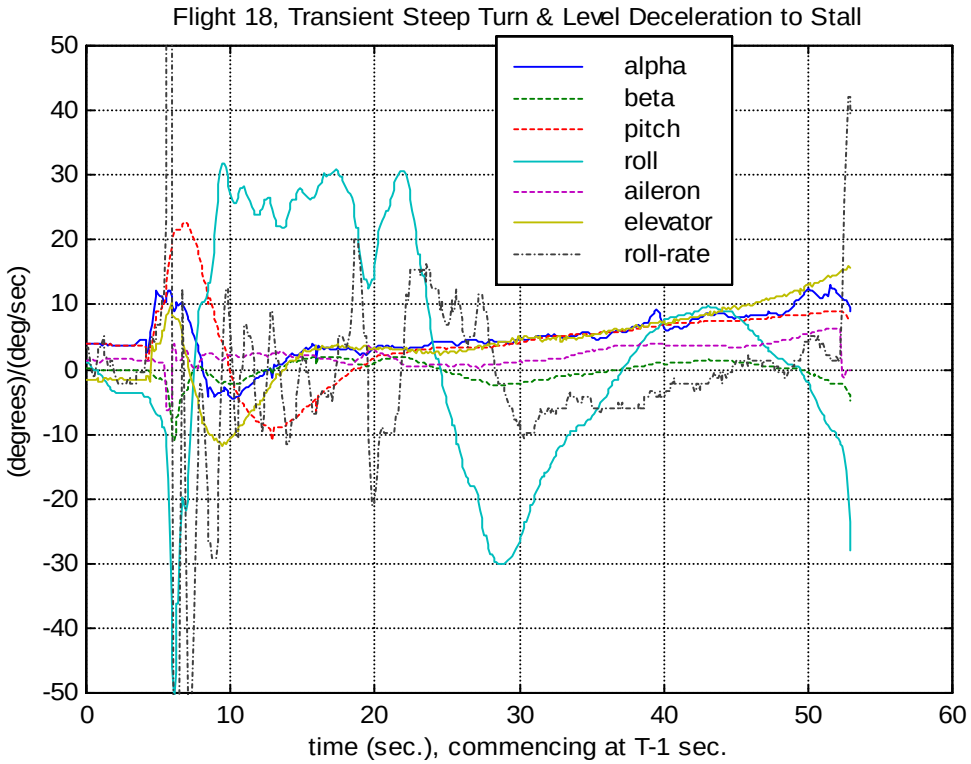

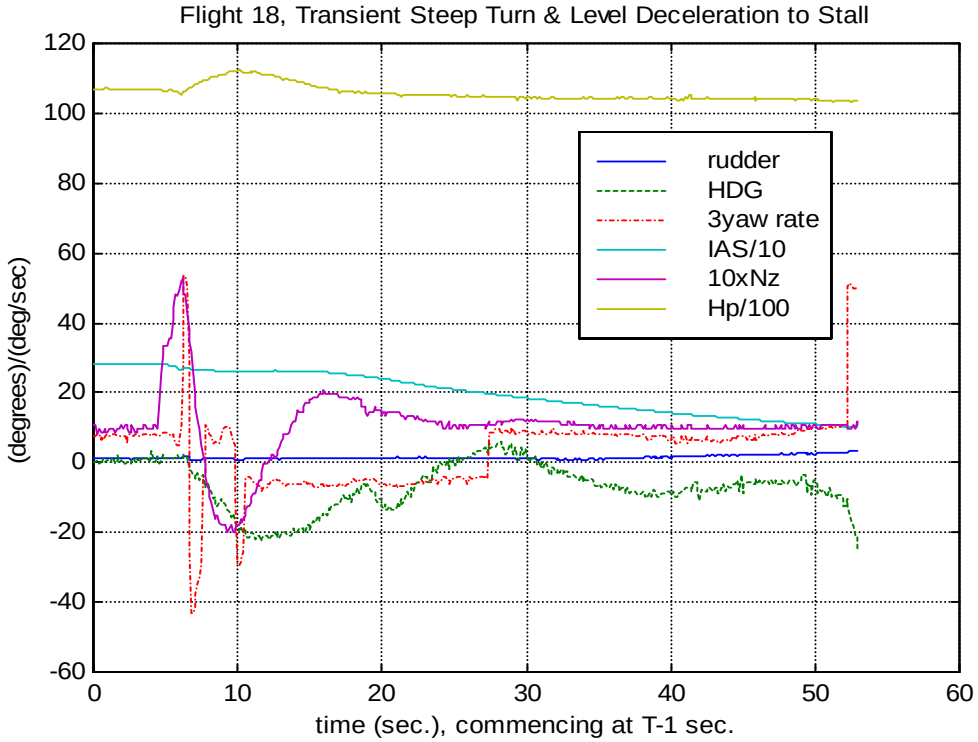

3.11.3.5 At the time of the above manoeuvres, the right 2LENS had been jettisoned, however the left 2LENS, although deployed, was most likely still being towed (accounting for the progressive aileron application, with reducing airspeed). Therefore, aerodynamically the wing was clean, with the exception of 6.4° aileron deflection at the stall. For this configuration, from the above figures, the calculated stall incidence, as defined above, was 13.1°, whilst the maximum incidence achieved during the transient steep turn was calculated to be 12.3°. The lack of definite pitch-break is significant, as it indicates an outboard stall, rather than wing-root / inboard stall. Recognising that, generally wing stores of appreciable size could be expected to reduce stall incidence, and likewise for aileron deflection, these figures indicate that the TPT17RF /TRX17DUMMY configuration mean launch peak incidence was possibly of the order of 85-90% of stall incidence.

3.11.4 Quasi-steady roll offset

3.11.4.1 The magnitude of the quasi-steady roll offset angle varied between configurations, and between launches of the same configuration. For example, for the TPT17RF/ TRX17 DUMMY configuration the quasi-steady roll offset angle varied between -8 and +16 degrees. The maintenance of the quasi-steady roll offset over a period of time was the primary reason for the large heading changes that occurred through many of the launch phases. In the case of FQT 20, the roll offset was 40°. The aileron angle was -4.5°, effectively at the limit of DAP-permitted authority, for the launch phase of flight. Not only was this an effective control limit condition, but a stability limit, because both $-L_P<0$ and $L_{\delta a}<0$, i.e. negative roll damping and reversed aileron effect, so that any additional disturbance (at that incidence) would lead to departure.

3.11.4.2 For the other flights, lesser aileron deflections were used to maintain the roll offset. With additional aileron deflection available, the DAP did not command additional aileron deflection, in an attempt to null the roll angle. It might be unwise to command additional aileron in this condition, because of the possibility of rendering $-L_p<0$ and $L_{\delta a}<0$, due to residual separated flow regions over the wing upper surface. Over the 'quasi-steady roll offset' segment of the launch phase, the aerodynamic parameters of interest are [incidence, sideslip, roll_(offset)_angle, aileron_deflection]. Examination of the reduced data indicates that sideslip was in the direction of the low wing, and that aileron opposed the low wing. This is indicative of a negative static lateral stability condition, or negative 'dihedral effect', an intrinsic aerodynamic stability parameter (as opposed to a DAP-imposed condition).

3.11.4.3 To study this possibility, parametric analysis has been conducted amongst the sub-set [aileron_deflection, incidence, roll_(offset)_angle]. The following figure shows the resultant parametric surface, obtained by numerical interpolation amongst the FQT data points. There are few 'quasi-steady roll offset' data points having roll_angle values greater than 15°; with few points in this regime, the numerical algorithm interpolates a planar surface. Therefore, for high roll_angle values, the interpolated surface should be viewed cautiously. The figure includes all configurations. It is seen that the parametric surface is reasonably planar (a few 'wrinkles' in the surface can be seen) and reasonably independent of incidence, although the above proviso must be noted. A tendency to be independent of incidence reflects a negligible change in sideslip stability derivatives over the range of incidence of the data set. In a quasi-steady roll-offset state, there is a balance between steady rolling moment due to aileron deflection and that due to lateral wing-lift distribution. Hence, the latter must be asymmetric. The planarity indicates reasonable linearity between the aileron_deflection and roll_(offset)_angle variables.

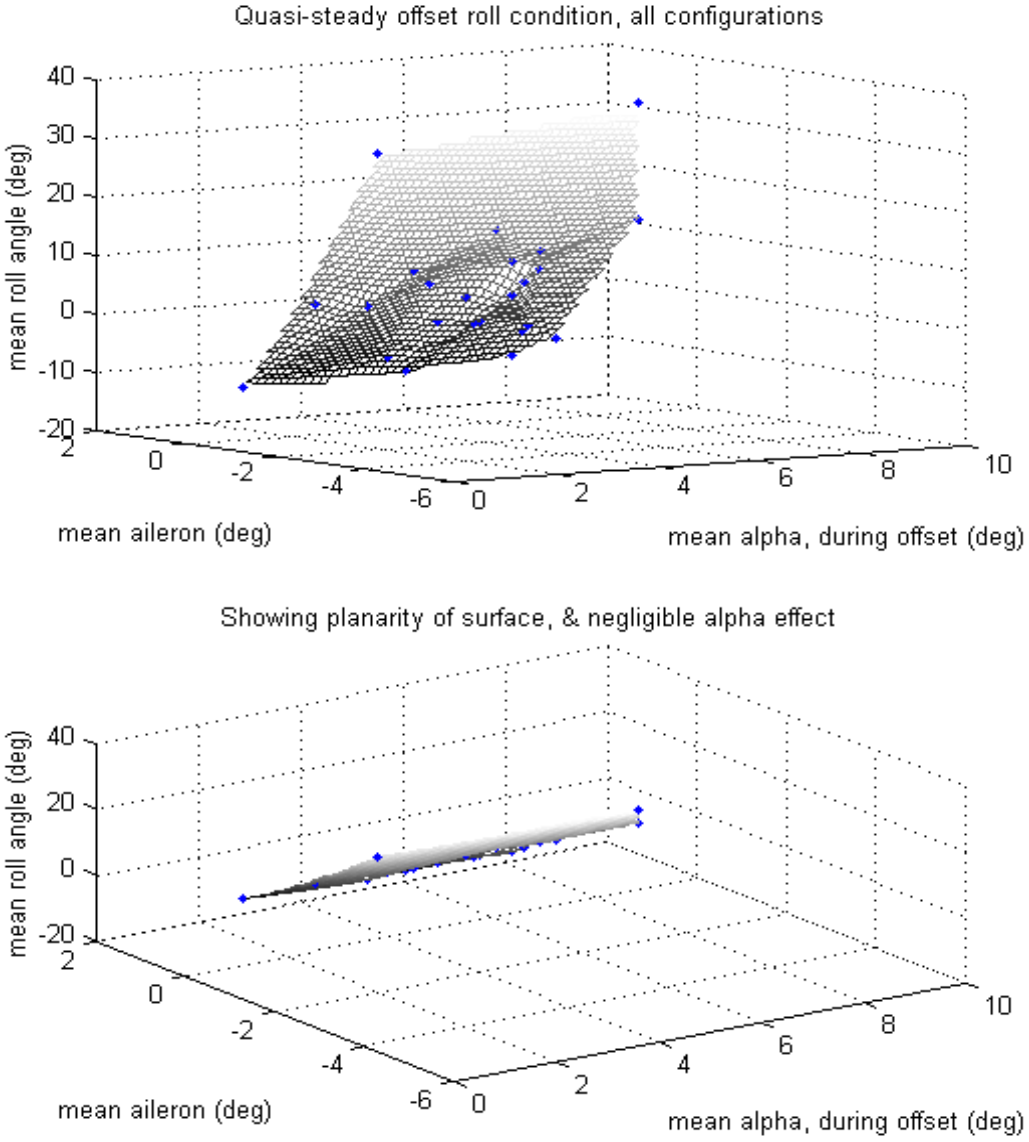

3.11.4.4 Quasi-steady aileron angles can be correlated against corresponding sideslip angles:

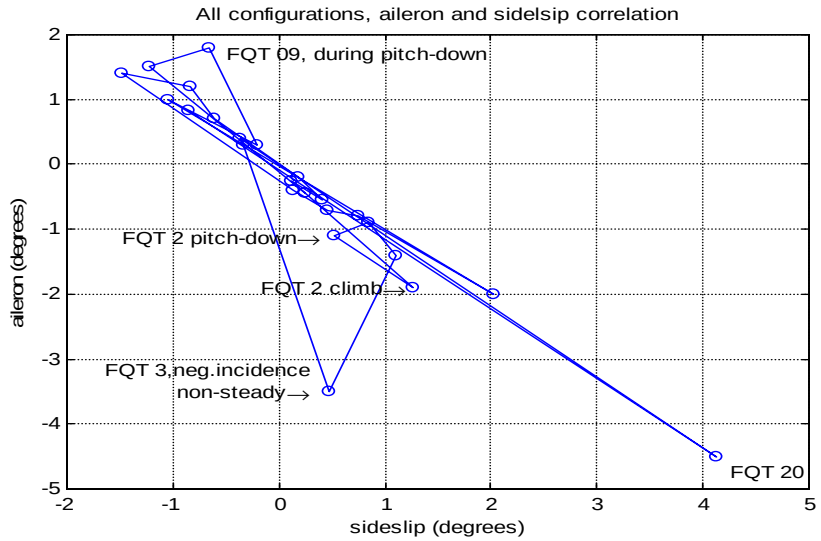

3.11.4.5 As seen from the above figure, with the exception of a limited number of FQT data points (FQT 2, 3, 9 and 20), there exists a linear relationship between aileron angle and sideslip angle. Furthermore, the aileron and sideslip angles are similar in magnitude. For the quasi-steady condition, given that roll rate and acceleration are approximately zero, the balance of rolling forces reduces to:

$$L_\beta \beta + L_{\delta a} \delta_a = 0$$

re-arranging,

$$L_\beta = -L_{\delta a} \frac{\delta_a}{\beta}$$

and, noting that $\delta_a \approx -\beta$,

$$L_\beta = L_{\delta a}$$

Noting that $L_{\delta a}>0$ normally (with a couple of exceptions, noted previously), $L_\beta>0$ also, of approximately the same magnitude as $L_{\delta a}$ - a markedly negative dihedral effect, or negative stick-free static lateral stability margin (normally $L_\beta<0$ for typical aircraft configurations, of perhaps 50% the magnitude of $L_{\delta a}$).

3.11.4.6 Wingsweep makes $-L_\beta$ strongly positive, whilst for a low-wing aircraft, fuselage effect has an incremental negative effect upon L_β; in the case of Kalkara, the engine pod would have a positive effect upon $-L_\beta$. These effects are inviscid. On the other hand, flow separation on the into-β wing, a viscous effect, also would have a negative incremental effect upon $-L_\beta$, as well as increasing the propensity for $-L_P<0$ and $L_{\delta a}<0$. If $-L_\beta<0$, the stick-free response is spiral divergence and low dutch roll damping, which was particularly observed on FQT 18. Both types of motion are *relatively* long period (although the spiral divergence time constant will reduce, the larger the magnitude of a negative $-L_\beta$) and should be satisfactorily controllable, with control laws that include a response to $-L_\beta$, by a DAP.

3.11.4.7 In the case of Kalkara, the aircraft has an oversized fuselage, in comparison to the wing-size. Therefore, the fuselage effect can be expected to provide a substantial negative increment to L_β. Whether this would be sufficient to overcome the positive increments due to wingsweep and engine pod, without the additional negative incremental effect from outboard flow separation, is a matter of experimental validation. Such experimental validation could be obtained from runway runs of a truck-mounted tufted aircraft.

3.11.4.8 The above analysis highlights the distinction between rolling motions occurring during the pitch-up phase of launch. Lower roll rates (less than perhaps 15 deg/sec) are indicative of a $-L_\beta<0$ response to yaw perturbations, whether crosswind-induced or RATO thrust-induced, whereas higher roll rates are induced by wing-flow separation, the effect of which is to establish a higher roll angle, by the time sufficient flow re-attachment has occurred to enable the DAP to satisfactorily dampen corrective roll overshoots and achieve a 'quasi-steady' condition. The higher offset roll angle is maintained by the DAP.

3.11.4.9 The reason for the maintenance of the offset roll angle by the DAP could possibly lie in the choice of the $C_{l\beta}$ numerical value in the dynamic model within the controlling algorithm of the DAP. As a difference between the MQM107E and Kalkara, the addition of the 'near-miss'

antennae on the wingtip upper and lower surfaces, could have introduced an additional negative increment to $-L_{\beta}$.

3.11.5 Variability of elevator deflection control

1.1.1.1 Inspection of the launch traces reveals a substantial variation in elevator deflection characteristics at the pitch-up check manoeuvre and the pitch-down check manoeuvre. In particular, elevator deflection exhibits a large variation in damping. For example, on FQT 10, N28-002 exhibited seven cycles of elevator deflection, before damping, whilst, on FQT 15, the same aircraft exhibited three cycles, and on FQT 20, an overdamped (the most desirable) pitch-up check deflection. Elevators exhibiting lowly-damped pitch-up check deflections also exhibited lowly-damped pitch-down check deflections. In all cases, the pitch-down check manoeuvre under-shot the pitch target, and was followed by a further pitch-down adjustment to achieve pitch/altitude targets.

3.11.5.2 The elevator deflection damping characteristics affected the peak positive incidence during pitch-up and the peak negative incidence, during pitch-down. The more lowly-damped the elevator deflection dynamic characteristics, the greater the peak positive and negative incidence values, and hence the less the margin against flow separation occurring from the upper and lower surfaces of the wings, respectively.

3.11.6 Anomalous Parameter Values

3.11.6.1 The FQT flight data traces reflect a number of parameter characteristics, which do not logically accord with expected characteristics:

a. *Yaw rate* - often, the yaw rate parameter values (presumably a digitised, and possibly processed signal, from the analogue output of the yaw rate gyroscope) do not reflect yaw rate, as assessed from the HDG parameter change (e.g. FQT 1, 3, 5, 13, 14, 15, 17, mostly the yaw rate parameter appears to be opposite in sign to yaw rate, although on FQT 1, the sign is the same, whilst, on FQT 18, there was no yaw rate parameter change, following T+3 seconds;

b. *HDG* - the HDG parameter has a particularly variable signal-to-noise ratio; FQT 17 exhibits a high noise content;

c. *Pitch angle* - following the completion of the pitch-over correction, and level altitude establishment, typically the pitch angle increases in magnitude as the aircraft accelerates; this could be reflective of a reduction in lift-curve-slope with increasing airspeed/Mach Number; generally, however, lift-curve-slope increases with increasing Mach Number, at least to the value of Mach Number at which viscous effects become significant.

3.12 Peak Incidence Margin to Stall Incidence

3.12.1 In order to account for flight path variabilities introduced by wind/atmospheric conditions, airframe structural production tolerances and component condition/performance, a sufficient margin needs to exist between peak incidence and stall incidence (defined as the incidence at which significant flow separation occurs), both positive, for the pitch-up check manoeuvre, and negative, for the pitch-down check manoeuvre. The ten flights in the TPT17RF/TRXDUMMY configuration have provided an indication of typical variability, namely

a standard deviation equates to ±13%. Wind strengths for this set of launches were a maximum of 20% of the headwind launch envelope and 50% of the crosswind launch envelope.

3.12.2 For a piloted fixed-wing aeroplane, the takeoff safety speed ($V_{2min}=1.2V_S$) margin to stall must be at least $1/\{1/1.2^2\}$, or 44% greater than takeoff safety incidence. Suggesting a manual-flight takeoff speed normal distribution, with a conservative standard deviation of $0.05V_S$, which equates to an incidence increment of 12% (quite similar to the present standard deviation), the margin, results in a stall incidence probability of exceedance of 10^{-4} (equating to 3.7 standard deviations). As the standard deviations are similar, this requires a similar probability of exceedance, i.e. a similar margin of 3.7 standard deviations margin, limiting the mean launch peak positive incidence to about 70% of stall incidence. Any lesser a margin requires a substantially more rigourous justification.

3.12.3 For the 'bunt', the pitch-down check manoeuvre, the margin can be less, primarily because of the up-and-away occurrence of the bunt.

3.13 Roll 'Offset' - Further Sideslip Analysis

3.13.1 Sideslip angles have been estimated, by assuming zero wind and by assuming the magnetometer HeaDinG indication is insensitive to pitch and roll angles. The combination of the two assumptions is tantamount to assuming the magnetometer heading was the track over the ground. Whereas, the effect of the assumptions upon estimated incidence is low-order, for the estimation of sideslip angles of small magnitude, the two assumptions can result in significant errors. Furthermore, zero magnetometer error has been assumed in the computations. In order to provide a further estimation, potentially of improved accuracy, additional analysis has been conducted, using the DGPS positional data.

3.13.2 To examine the potential of such additional analysis, FQT 14 has been analysed, because the flight was conducted in 'calm' surface wind conditions. For the analysis, the DGPS lat/long data was low-pass filtered, phase-corrected, numerically-differentiated, with respect to each other for true heading derivation, adjusted for magnetic variation, aligned to the magnetometer indication near-launch to account for system error, and numerically-differenced for ground speed estimation. Zero wind variation with altitude was assumed.

3.13.3 The recorded DGPS lat/long data is shown below, raw-acquired and filtered:

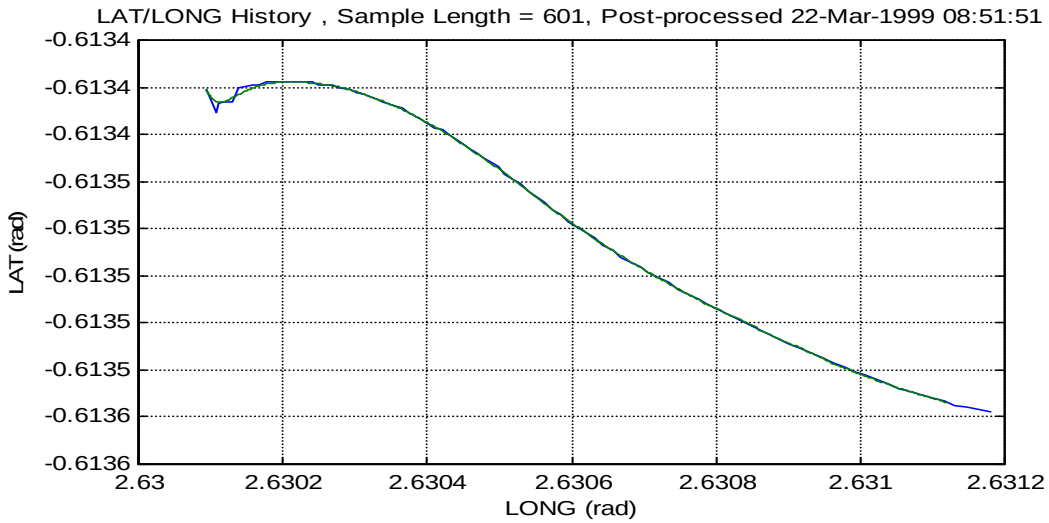

For the first four seconds of the flight (i.e., through the large horizontal acceleration phase of flight), no reliable DGPS information was obtained. From the data, the computed heading, corrected for phase-adjustment, magnetic variation and assumed magnetometer system error, in order to align, is shown below, together with the computed ground speed:

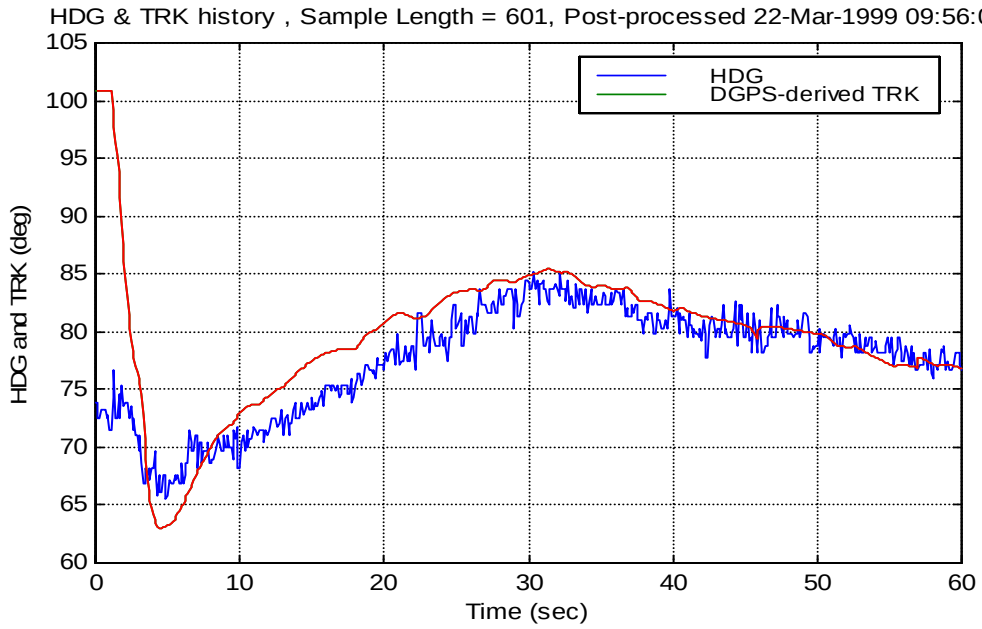

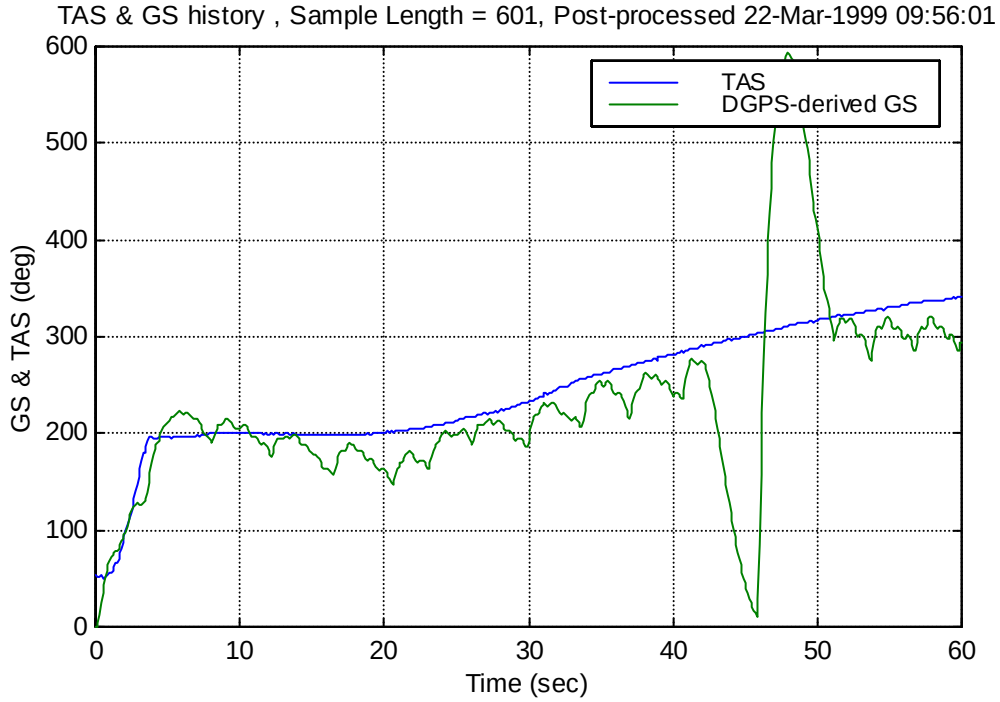

3.13.4 The ground-speed anomaly is indicative of a partial DGPS dropout at some time during the period between T+42 and T+49, and is typical of the DGPS-derivation of velocity. Further processing, in order to bridge the dropout, has not been conducted presently. Assuming zero wind throughout the 2200 feet height of the launch phase, the earth-fixed along-track and across-track velocity components, relative to the initial launch direction, have been computed, using aircraft DGPS-derived heading. As before, the inverse Euler transformation has been computed, using the magnetometer HDG, in order to transform the earth-axes velocity components, to the aircraft-axis system, and hence incidence and sideslip values. Basically, the

larger the difference between DGPS-derived heading and magnetometer HDG, the greater the sideslip angle.

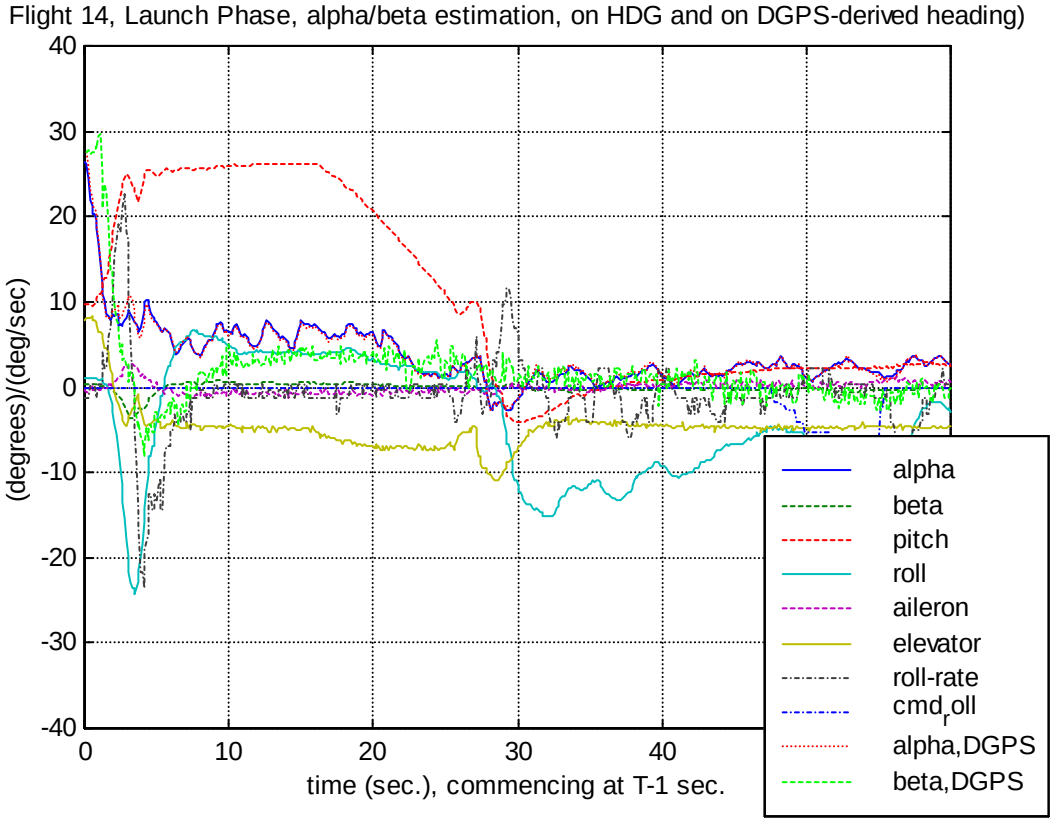

3.13.5 It is seen that, over the 'offset' roll segment of the launch phase of flight, the process has estimated a positive angle of sideslip of larger magnitude, than the HDG-alone method of estimation, used previously. Over the 'offset' roll segment of the flight, the so-computed mean sideslip angle was 3.2°, compared to the roll angle of 4.3°, and the earlier estimation of sideslip, 0.5°. The larger value of sideslip is equivalent to a less negative dihedral effect, $-C_{l\beta}$, stick-free static lateral stability parameter.

3.13.6 Similar analyses have been conducted for other low surface wind launches, namely FQT 18 and 20; for FQT 18,

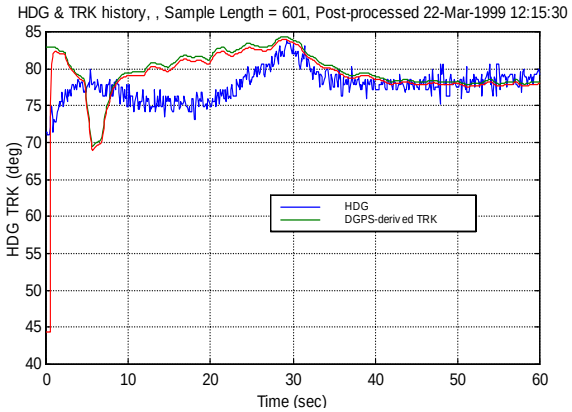

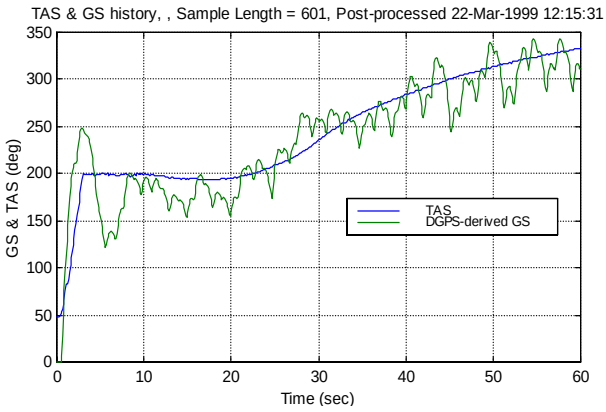

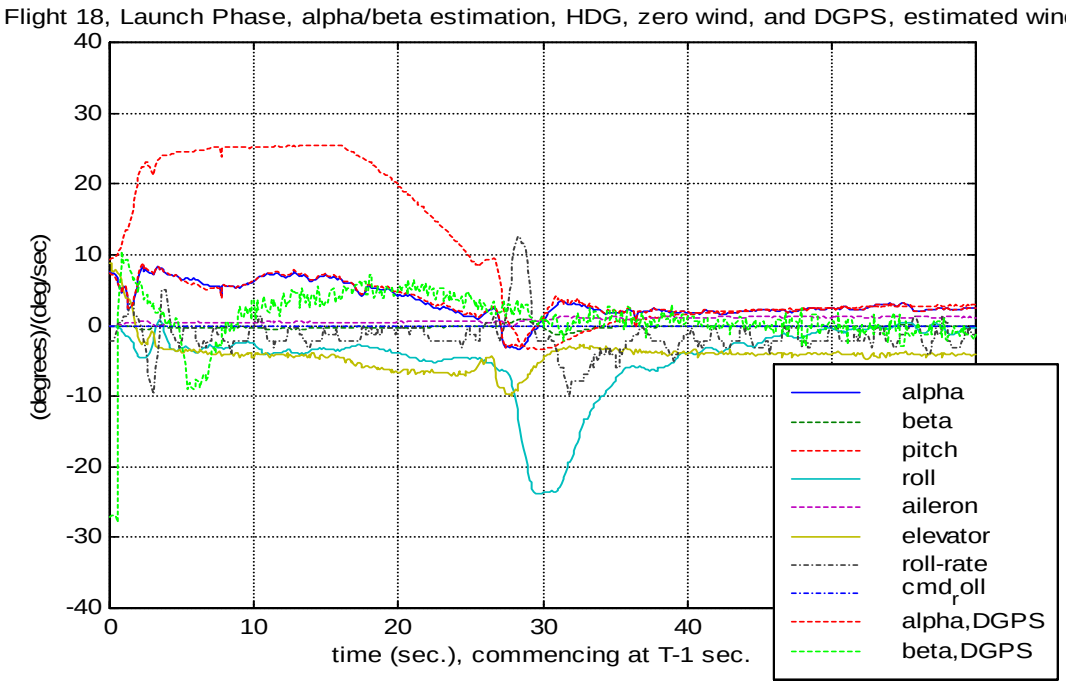

3.13.7 Similarly to FQT 14, the reduced data for FQT 18 shows a positive sideslip condition during the quasi-steady offset-roll condition, a mean value of 2.5°, compared to -0.3°, previously. For FQT 20:

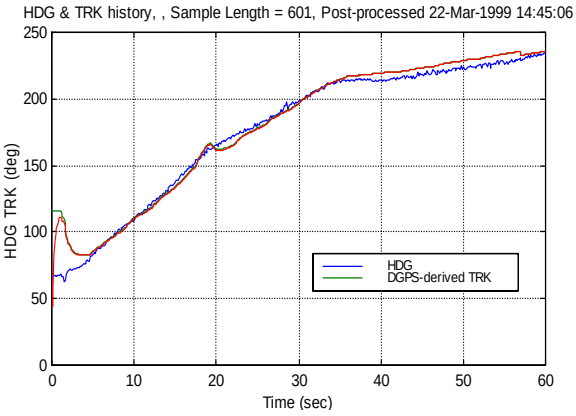

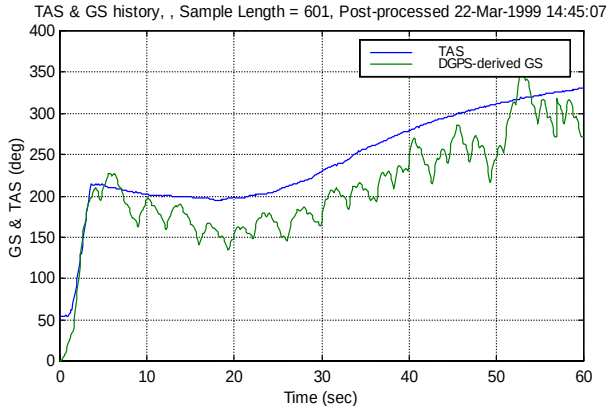

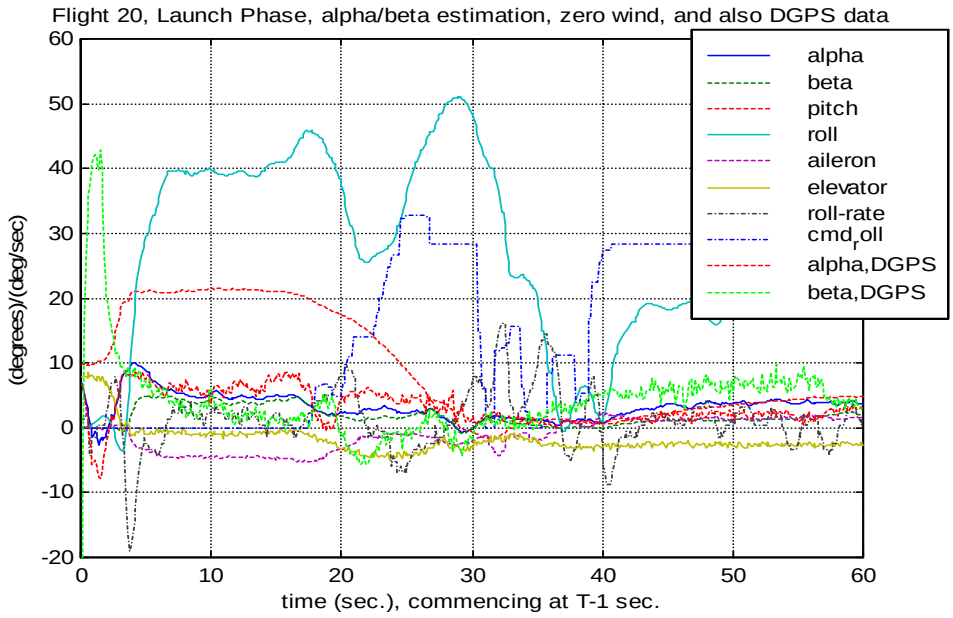

1.1.8 Over the quasi-steady roll offset roll segment of the FQT 20, launch, the DGPS-reduced sideslip has a mean value of 2.1°, compared with the formerly estimated value of 3.9°. The incidence, after the initial peak, is estimated to be 2-4° greater than the former estimation. At T+14, the incidence rises by about 2°, to approximately 9°, the same magnitude as the estimated initial peak. This rise coincides with the onset of negative $L_{\delta a}$, reverse aileron effect, indicative of increased flow separation over the aileron, and is therefore physically realistic. Considering a flight with a non-zero surface wind, FQT 08:

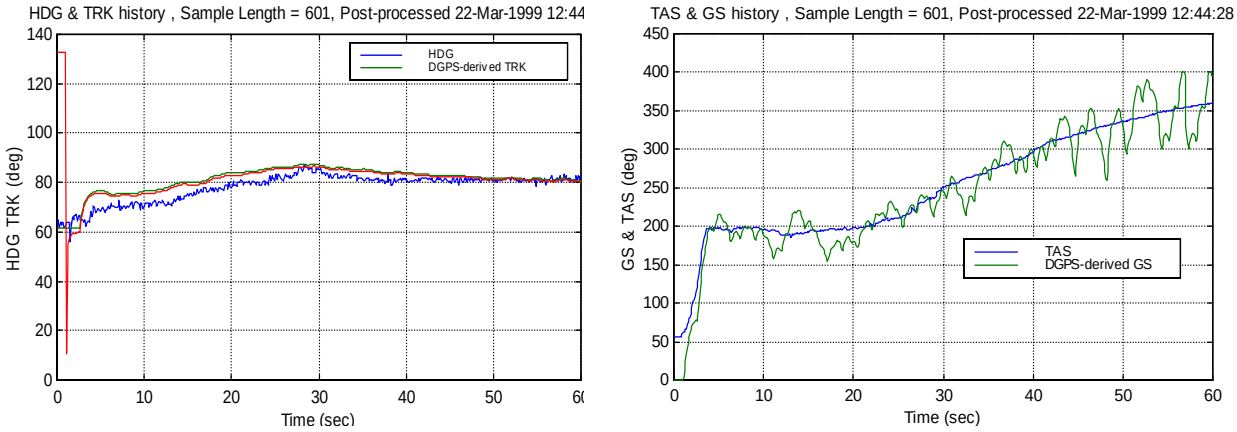

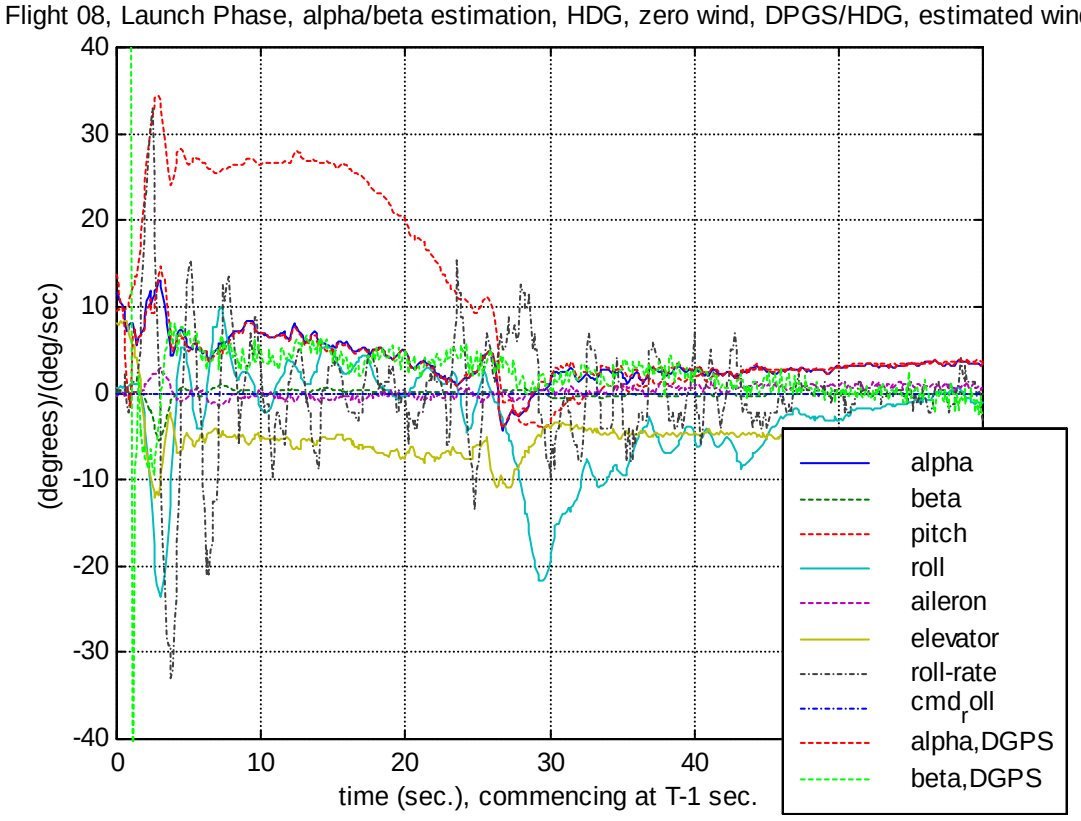

3.13.9 For the non-zero surface wind condition, no change in wind direction with height is assumed, and a $1/7^{th}$ power-law is assumed, for the variation of wind magnitude with height. For the quasi-steady roll offset roll segment of the FQT 08 launch, the DGPS-reduced sideslip has a mean value of 4.2°, compared with the formerly estimated value of 0.2°. The large difference is symptomatic of the greater errors introduced by assuming no change in wind direction, with height, and a $1/7^{th}$ power-law assumption, for the variation in wind magnitude, with height. Some of the other low wind FQTs, some with significant surface wind, have been similarly analysed:

For FQT 09, surface wind 260/04 knots:

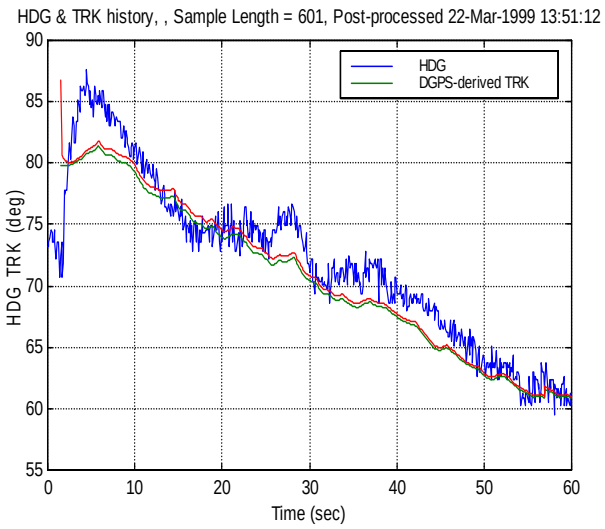

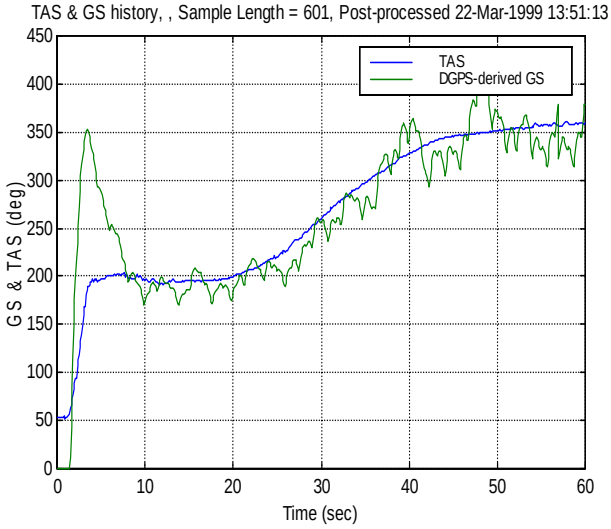

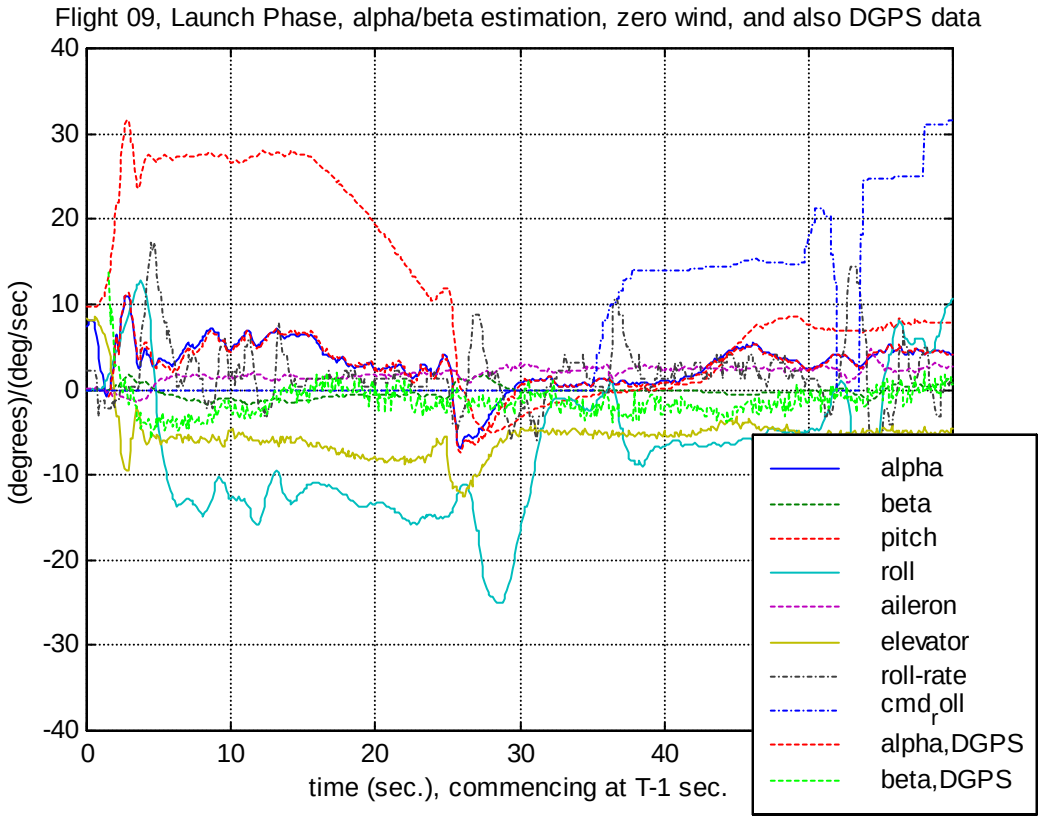

For FQT 11, surface wind 080/08 knots:

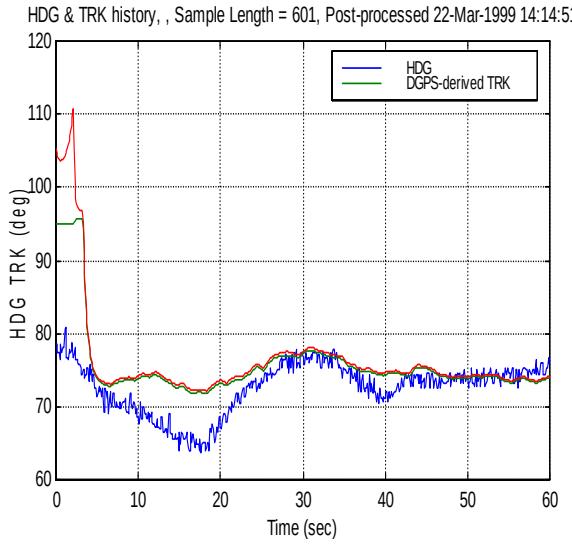

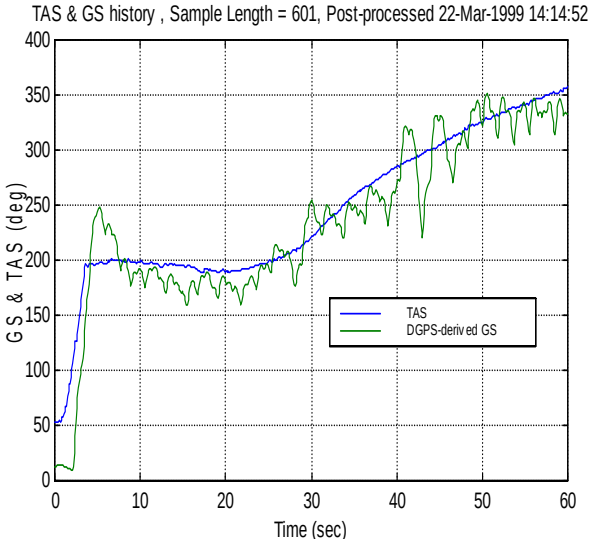

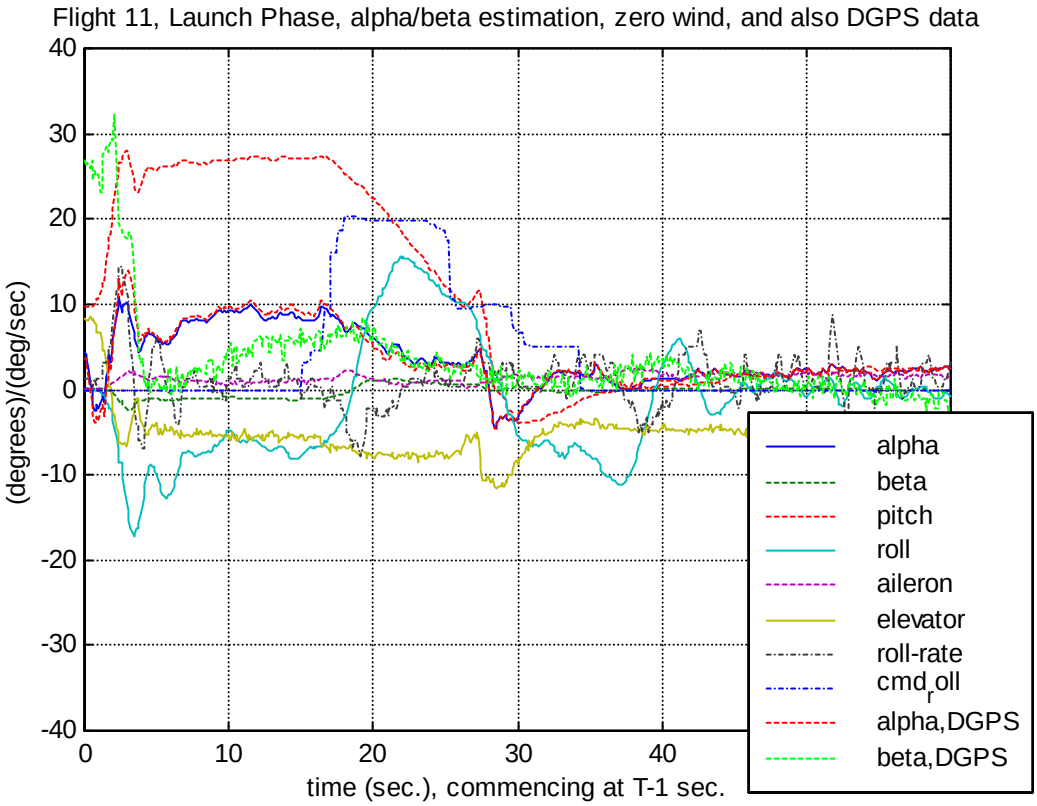

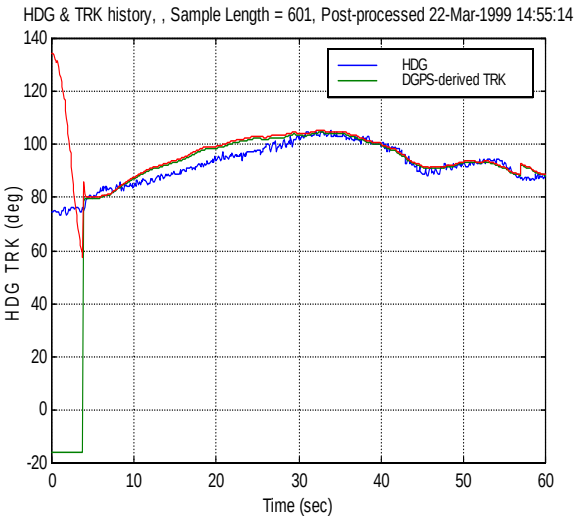
HDG & TRK history, , Sample Length = 601, Post-processed 22-Mar-1999 14:55:14
HDG
DGPS-derived TRK
HDG TRK (deg)
Time (sec)

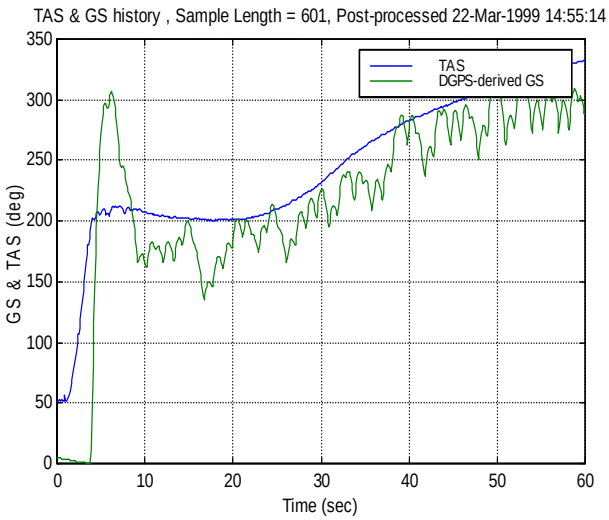
TAS & GS history , Sample Length = 601, Post-processed 22-Mar-1999 14:55:14
TAS
DGPS-derived GS
GS & TAS (deg)
Time (sec)

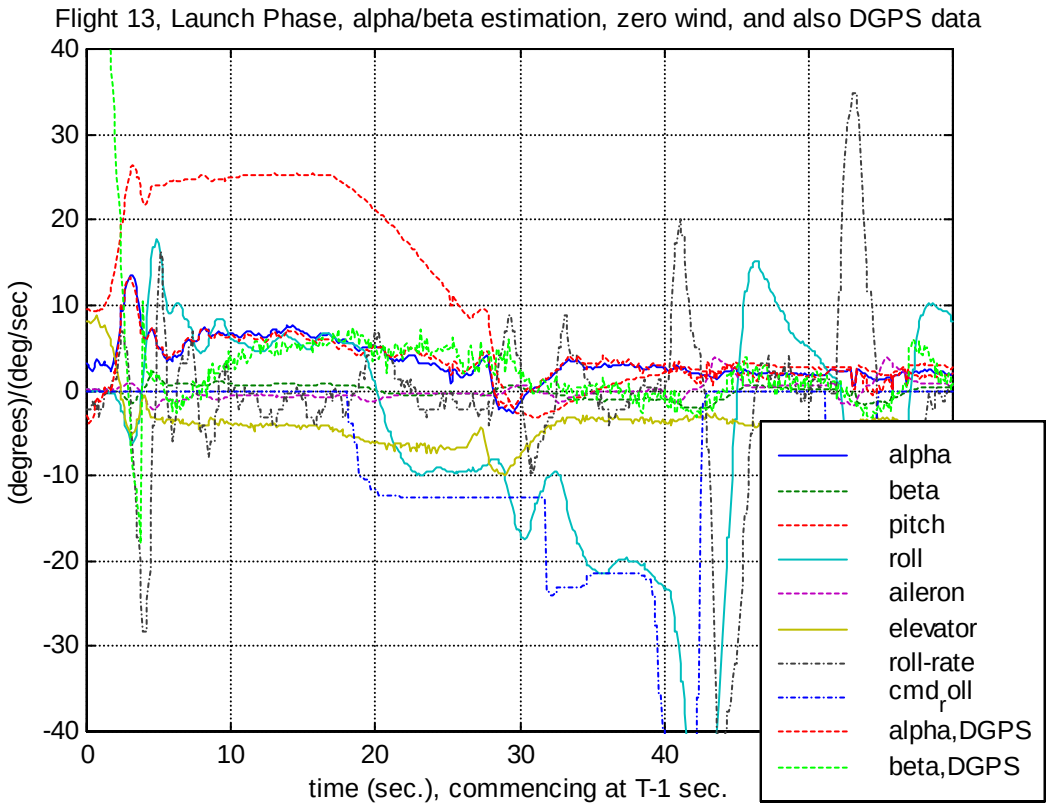
Flight 13, Launch Phase, alpha/beta estimation, zero wind, and also DGPS data
(degrees)/(deg/sec)
time (sec.), commencing at T-1 sec.
alpha
beta
pitch
roll
aileron
elevator
roll-rate
cmd_roll
alpha,DGPS
beta,DGPS

3.13.10 For the majority of flights, e.g. FQT 11, 13, 14, 18 and 08, the DGPS-computed track is to the right of the HDG. With due regard to the local wind variations about the Jervis Bay peninsula, and the possible wind variation with height, this could also be indicative of a wind effect, to some extent, but unlikely, to the extent computed, due to the low surface wind-speed at the aerodrome. Therefore, the DGPS analysis indicates that, during the quasi-steady offset roll (i.e. climb) segment of the launch phase, the aircraft was generally in a right sideslip state. When correlated against quasi-steady aileron deflection (see the following figure), the estimated sideslip data shows greater scatter than the previous estimated sideslip values (the usage of DGPS data, earth-referenced as it is, with assumed wind vectors, introduces errors due to actual wind profiles, unlike the usage of air data, alone, which neglects all wind effects):

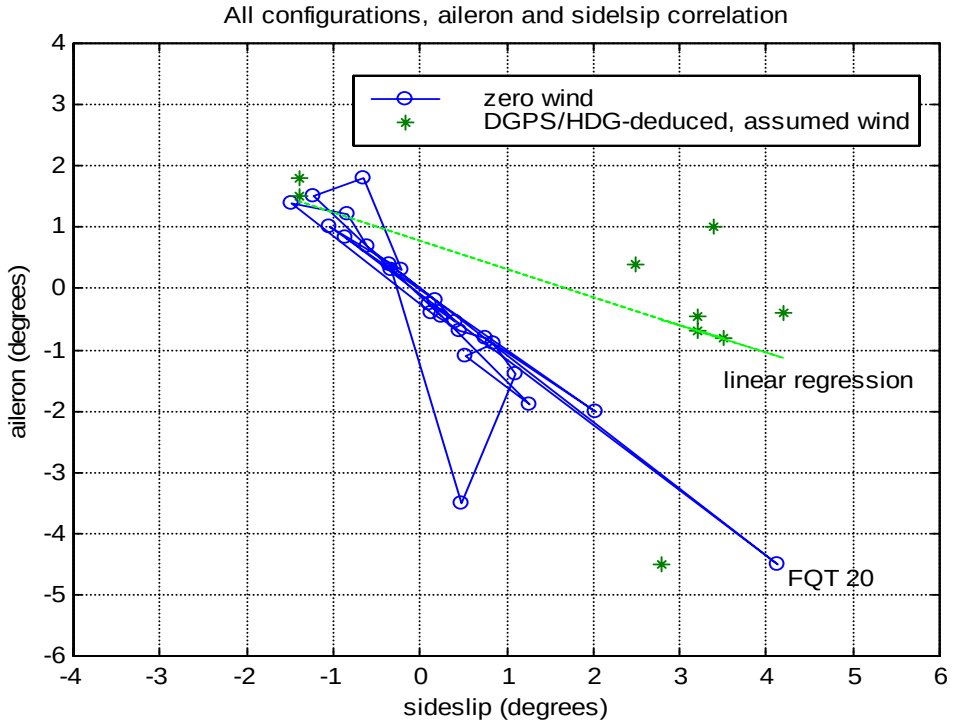

3.13.11 In spite of the greater scatter, the trend of the sideslip/aileron relationship indicates a negative dihedral effect, $C_{l\beta}$.

4. CONCLUSIONS

1.1.1 A series of launches of the same nominal Kalkara configuration has illustrated a significant degree of variability, which could be attributable to launch wind/atmospheric conditions, airframe tolerances and component condition/performance, amounting to a standard deviation of 13% of mean peak incidence.

4.1.2 The high-roll-rate uncontrolled rolls at launch pitch-up, or shortly thereafter, are symptomatic of outboard loss of lift and wing roll damping, due to outboard/wingtip flow separation. For the same store configuration, the roll acceleration and roll rate generally varied directly with peak incidence.

4.1.3 With reducing incidence, the DAP was generally able to stabilise transient motions to 'quasi-steady' conditions. However, with the aircraft in a 'quasi-steady' state, the DAP maintained an offset roll angle, largely responsible for the progressive turn of the aircraft through the launch

phase. The magnitude of the offset roll angle varied directly with the magnitude of the pitch-up rolling motions, and, hence, peak incidence.

4.1.4 On FQT 20, the aircraft was on the limit of controllability throughout the launch phase, as evidenced by a reversed response ($L_{\delta a}<0$) to aileron input.

4.1.5 Zero wind analysis of the 'quasi-steady' flight conditions reveals a linear and reasonably constant dihedral effect, or stick-free static lateral stability derivative. The derivative, L_{β}, was of the same sign and similar magnitude as the aileron power derivative, $L_{\delta a}$, indicating that the aircraft possessed a markedly negative stick-free static lateral stability margin. A second analysis, using an assumed vertical wind profile, from recorded surface wind, supports the negative stick-free static lateral stability margin deduction, although of a lesser magnitude.

4.1.6 During the pitch-down check manoeuvre, at the completion of climb, incidence peaked at negative values. Responsively, uncommanded rolling motions occurred, indicative of significant wing lower surface flow separation occurring.

4.1.7 Elevator deflection characteristics during the pitch-up and pitch-down check manoeuvres exhibited a large variability of damping. Generally, the lower the damping ratio, the greater the values of peak positive and negative incidence.

4.1.8 The yaw rate parameter exhibited anomalous characteristics on several flights. The noise to signal ratio of the HDG parameter was variable, and, often, excessive. The pitch angle parameter displayed an increase during accelerating level flight, following the completion of the climb.

5. RECOMMENDATIONS

5.1.1 As part of the due process of Type Certification, the present launch characteristics of Kalkara have a significant impact upon the system safety and hazard analysis, and require resolution. For such a resolution, a number of actions are recommended.

5.1.2 The positive and negative stall incidence of the Kalkara aircraft, in all configurations, should be experimentally estimated, in the first instance, by captive-testing, truck-mounted, along the runways at the Jervis Bay Range Facility, and the nature and extent of upper and lower surface flow separation mapped, accordingly, in order to determine the stall margin, during launch pitch-up. The effects of aileron gap-seals and wingtip 'near-miss' antennae should be determined.

5.1.3 If insufficient margin against wing-flow separation is likely to exist, aerodynamically, it would be preferable to undertake an aerodynamic improvement programme for the wing (for example, using vortex generators and fences), in order to control flow separation, and delay stall incidences. In addition, the launch configuration could be analysed and adjusted (RATO angle and elevator initial angle), so that the margin is further increased. As the elevator deflection damping characteristics affect the peak incidence values, the variability of damping and frequent occurrence of low damping should be investigated.

5.1.4 Subsequently, all flights should be conducted in still-air conditions, in order to quantify the variability of launch peak incidence and dynamic behaviour, without any wind or atmospheric effects.

5.1.5 Such flights should include level deceleration manoeuvres, to the incipient stall, in order to determine and validate the stall incidences, estimated by captive ground tests.

5.1.6 An investigation into the roll-offset phenomenon should be conducted. The phenomenon may a result of aerodynamic hysteresis, residual separated flow reducing aileron effect and, simultaneously, reducing static lateral stability to a negative value. Furthermore, the vehicle modelling and controlling algorithms of the DAP should be examined, in order to ascertain the modelling and/or inclusion nature of a dihedral effect derivative, $C_{l\beta}$. It is possible that, compared to the MQM107E, the magnitude of the derivative has been increased by the presence of the 'near-miss' wingtip antennae.

5.1.7 The adequacy of the Electrical Sub-system Test Procedures should be reviewed, in relation to the sufficiency and ability of the tests, to capture partial serviceability, or pending unserviceability, of critical flight sub-system LRUs, in particular the yaw rate gyro and magnetometer. Such a review would support the different regular operational environment of Kalkara, when compared to that of MQM107E, and the impact of the environment upon the reliability of system components.